Hindawi
Oxidative Medicine and Cellular Longevity
Volume 2023, Article ID 9803148, 1 page
https://doi.org/10.1155/2023/9803148

Retraction

Retracted: Identification of HIBCH as a Fatty Acid Metabolism-Related Biomarker in Aortic Valve Calcification Using Bioinformatics

Oxidative Medicine and Cellular Longevity

Received 26 December 2023; Accepted 26 December 2023; Published 29 December 2023

This article has been retracted by Hindawi, as publisher, following an investigation undertaken by the publisher [1]. This investigation has uncovered evidence of systematic manipulation of the publication and peer-review process. We cannot, therefore, vouch for the reliability or integrity of this article.

Please note that this notice is intended solely to alert readers that the peer-review process of this article has been compromised.

Wiley and Hindawi regret that the usual quality checks did not identify these issues before publication and have since put additional measures in place to safeguard research integrity.

We wish to credit our Research Integrity and Research Publishing teams and anonymous and named external researchers and research integrity experts for contributing to this investigation.

The corresponding author, as the representative of all authors, has been given the opportunity to register their agreement or disagreement to this retraction. We have kept a record of any response received.

References

[1] J. Chen, Y. Sun, T. Xiong, G. Wang, and Q. Chang, "Identification of HIBCH as a Fatty Acid Metabolism-Related Biomarker in Aortic Valve Calcification Using Bioinformatics," *Oxidative Medicine and Cellular Longevity*, vol. 2022, Article ID 9558713, 24 pages, 2022.

Hindawi
Oxidative Medicine and Cellular Longevity
Volume 2022, Article ID 9558713, 24 pages
https://doi.org/10.1155/2022/9558713

Research Article

Identification of HIBCH as a Fatty Acid Metabolism-Related Biomarker in Aortic Valve Calcification Using Bioinformatics

Jun-Yu Chen,[1] **Ya-Ru Sun**,[2] **Tao Xiong**,[1] **Guan-Nan Wang**,[3] **and Qing Chang**[1]

[1]*Department of Cardiovascular Surgery, The Affiliated Hospital of Qingdao University, Qingdao University, Qingdao, Shandong 266003, China*
[2]*Department of Nursing, School of Nursing, Qingdao University, Qingdao, Shandong 266000, China*
[3]*Department of Pediatric Oncology, Affiliated Cancer Hospital of Shandong First Medical University, Jinan, Shandong 250117, China*

Correspondence should be addressed to Qing Chang; changqing20671@qdu.edu.cn

Received 29 July 2022; Revised 17 September 2022; Accepted 22 September 2022; Published 7 October 2022

Academic Editor: Md Sayed Ali Sheikh

Objective. To identify fatty acid metabolism-related biomarkers of aortic valve calcification (AVC) using bioinformatics and to research the role of immune cell infiltration for AVC. *Methods.* The AVC dataset was retrieved from the Gene Expression Omnibus database. R package is used for differential expression genes analysis and weighted gene coexpression analysis. The differentially coexpressed genes were identified by the Venn diagram, followed by Gene Ontology (GO) and Kyoto Encyclopedia of Genes and Genomes (KEGG) enrichment analyses of differentially coexpressed genes. Functions closely related to AVC were identified by GO and KEGG enrichment analyses of differentially coexpressed genes. Genes related to fatty acid metabolism were retrieved from the Molecular Signatures Database (MSigDB) database. After removing duplicate genes, least absolute shrinkage and selection operator (LASSO) regression analysis, support vector machine recursive feature elimination (SVM-RFE), and random forest were applied to recognize biomarkers related to fatty acid metabolism in AVC. The CIBERSORT tool was used to analyze infiltration of immune cells in normal and AVC samples. Correlations between biomarkers and immune cells were calculated. Finally, HIBCH-related pathway was predicted by single-gene gene set enrichment analysis (GSEA). *Results.* 2416 differentially expressed genes and one coexpression module were identified. A total of 1473 differentially coexpressed genes were acquired. GO and KEGG enrichment analyses demonstrated that differentially coexpressed genes were closely related to fatty acid metabolism. LASSO regression analysis, SVM-REF, and random forest revealed that 3-hydroxyisobutyryl-CoA hydrolase (HIBCH) was a biomarker of fatty acid metabolism-related genes in AVC. Significant high levels of memory B cells were found in AVC than normal samples, while activated natural killer (NK) cells were significantly low in AVC than normal samples. A significantly positive relevance was observed between HIBCH and activated NK cells, regulatory T cells, monocytes, naïve B cells, activated dendritic cells, resting memory CD4 T cells, resting NK cells, and CD8 T cells. A significantly negative relevance was observed between HIBCH and activated memory CD4 T cells, memory B cells, neutrophils, gamma delta T cells, M0 macrophages, and plasma cells. The single-gene GSEA results suggest that HIBCH may work through the inhibition of multiple immune-related pathways. *Conclusion.* HIBCH is closely relevant to immune cell infiltration in AVC and could be applied as a diagnostic marker for AVC.

1. Introduction

Aortic valve calcification (AVC) is an increasingly common condition affecting approximately 12.6 million people each year, of which more than 2% of people are about 70 years old [1]. A healthy aortic valve ensures unidirectional blood flow, which opens during systole and closes during diastole. However, in patients with AVC, the valve has reduced mobility due to overlying calcified nodules, obstruction of the left ventricular outflow tract, and blocking of cardiac

Table 1: AVC and normal sample information.

Series	Number of AVC samples	Number of normal samples	Platform
GSE12644	10	10	[HG-U133_Plus_2] Affymetrix Human Genome U133 Plus 2.0 Array
GSE51472	10	5	[HG-U133_Plus_2] Affymetrix Human Genome U133 Plus 2.0 Array
GSE83453	9	8	Illumina HumanHT-12 V4.0 expression beadchip
GSE153555	11	10	Illumina HiSeq 2500 (Homo sapiens)

output, impairing the patient's ability to exercise. This leads to left ventricular hypertrophy, which ultimately culminates in heart failure and possibly death [2–4].

Recent histopathological studies have shown that AVC is involved in lipid infiltration, inflammation, and calcification. It also has numerous clinical risk factors in common with atherosclerosis. In addition, it is likely another manifestation of atherosclerosis [5]. AVC may be closely linked to lipid metabolism. However, the etiology and causes of AVC progression have not been fully elucidated. There are no drugs available to prevent or stop the progression of AVC [6]. Further, surgery is the only effective treatment that can improve the clinical symptoms of AVC patients [7]. However, surgical treatments are costly and have high mortality rates. Further, the prosthetic valve gradually fails over time since the cause of the disease is not addressed. These factors continue to stress patients [8].

Therefore, more researches are required to explore the pathogenesis of AVC and potential therapeutic targets. The advancement in high-throughput sequencing technology, publicly available databases like Gene Expression Omnibus (GEO), and bioinformatics aid in the discovery of biomarkers and therapeutic targets associated with AVC pathogenesis. In this study, differentially expressed genes (DEGs) analysis, weighted gene coexpression network analysis (WGCNA), LASSO regression analysis, SVM-REF, and random forest were used to identify AVC biomarker signature. We investigated the difference in immune cell infiltration between normal and AVC samples. Further, the relation between AVC biomarkers and immune cell infiltration was analyzed by the cell-type identification by estimating relative subsets of RNA transcripts (CIBERSORT) tool.

2. Materials and Methods

2.1. Data Download and Processing. Four AVC datasets, GSE12644, GSE51472, GSE83453, and GSE153555, were retrieved from the GEO database (https://www.ncbi.nlm.nih.gov/gds/) for analysis. GSE12644 and GSE51472 were combined and used as the training group, and GSE83453 and GSE153555 were used as the test group. The platform and the number of samples included in each series are shown in Table 1.

2.2. Differentially Expressed Gene Analysis and WGCNA. The linear models for microarray data "limma" [9] R package were used to identify the DEGs between the AVC and the normal samples and to plot the heatmap. DEGs with $P < 0.05$ were considered statistically significant. The smallest number of genes in the module is set to 60, and the "WGCNA" R package [10] was employed to build a coexpression network for the combined datasets (GSE12644 and GSE153555).

2.3. GO and KEGG Enrichment Analyses of Differentially Coexpressed Genes. Using Venny 2.1.0 (https://bioinfogp.cnb.csic.es/tools/venny/index.html), the intersection of DEGs with genes in the module with the highest relevance to AVC in WGCNA is considered as differentially coexpressed genes. GO and KEGG enrichment analyses of differentially coexpressed genes were achieved using the "clusterProfiler" [11] R package.

2.4. Screening for AVC Fatty Acid Metabolism-Related Biomarkers. Three fatty acid metabolism-related gene sets were obtained from the MSigDB, (http://www.gsea-msigdb.org/gsea/msigdb/index): HALLMARK_FATTY_ACID_METABOLISM, KEGG_FATTY_ACID_ METABOLISM, and REACTOME_FATTY_ACID_METABOLISM, and duplicate genes were removed using Venny2.1.0. A Venn diagram was created to screen for fatty acid metabolism-related genes among the differentially coexpressed genes. LASSO regression, SVM-REF [12], and random forest [13] analyses were performed using the "glmnet" [14, 15], "e1071" [16], and "randomForest" R package, respectively, to identify AVC-related biomarkers. Finally, the "pROC" R package [17] was used to calculate the area under the curve (AUC) of the receiver operating characteristic (ROC) to assess the diagnostic efficiency of biomarkers.

2.5. Immune Cell Infiltration Analysis. The CIBERSORT [18] tool was used to determine the content of 22 immune cells and plotted using the "vioplot" R package. The correlation heatmap was created using the "corrplot" R package. Subsequently, the connection between AVC biomarkers and infiltration of immune cells was analyzed by Spearman's rank test.

2.6. Single-Gene GSEA. Single-gene GSEA was carried out in AVC patients using the combined GSE12644 and GSE51472 datasets. AVC patients were grouped into two groups based on their median HIBCH expression: those with high HIBCH expression groups and those with low HIBCH expression groups. The software GSEA 4.1.0 and gene set "c2.cp.kegg.v2022.1.Hs.symbols.gmt" were applied to analysis.

3. Results

3.1. Differentially Expressed Gene Analysis and WGCNA. GSE12644 and GSE51472 datasets were merged and

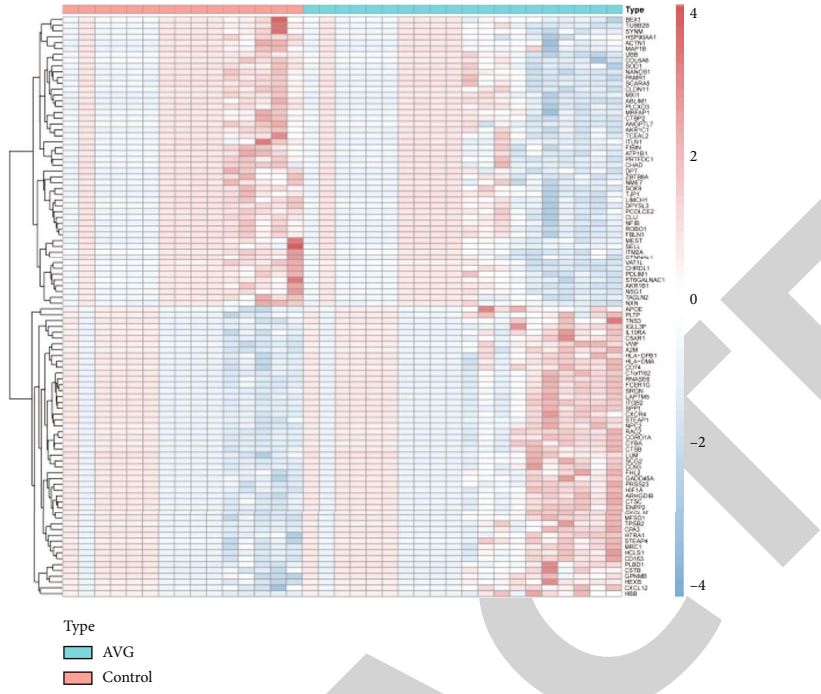

(a)

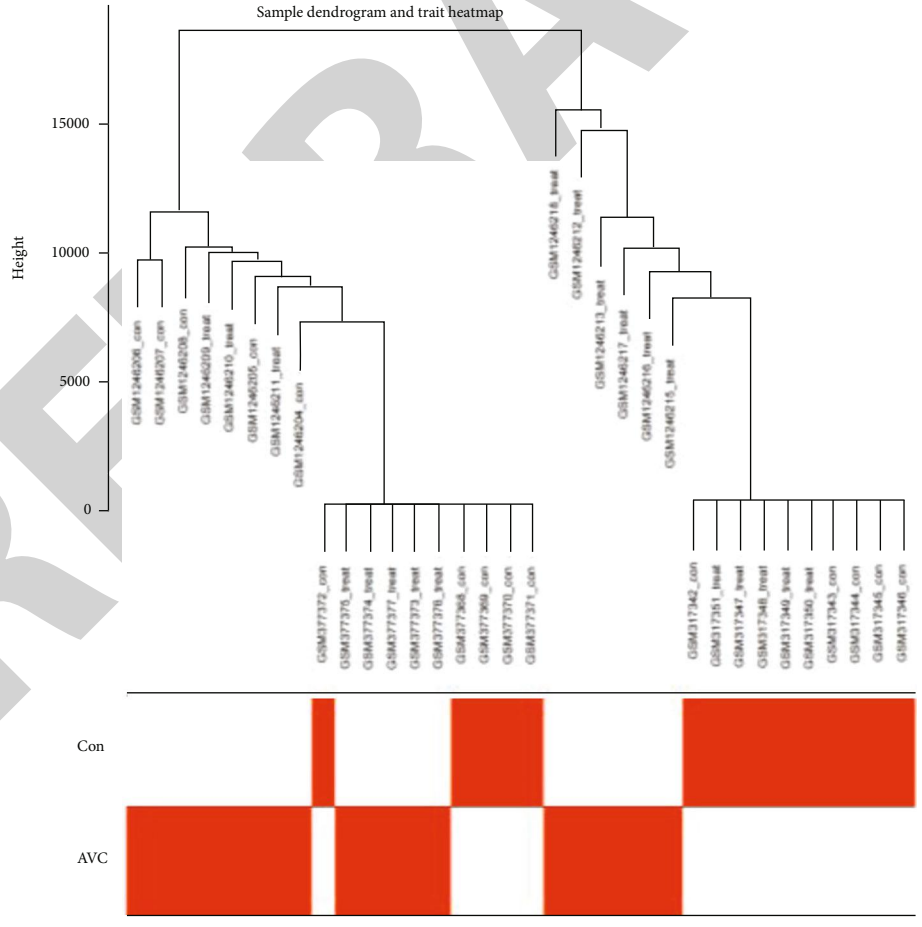

(b)

Figure 1: Continued.

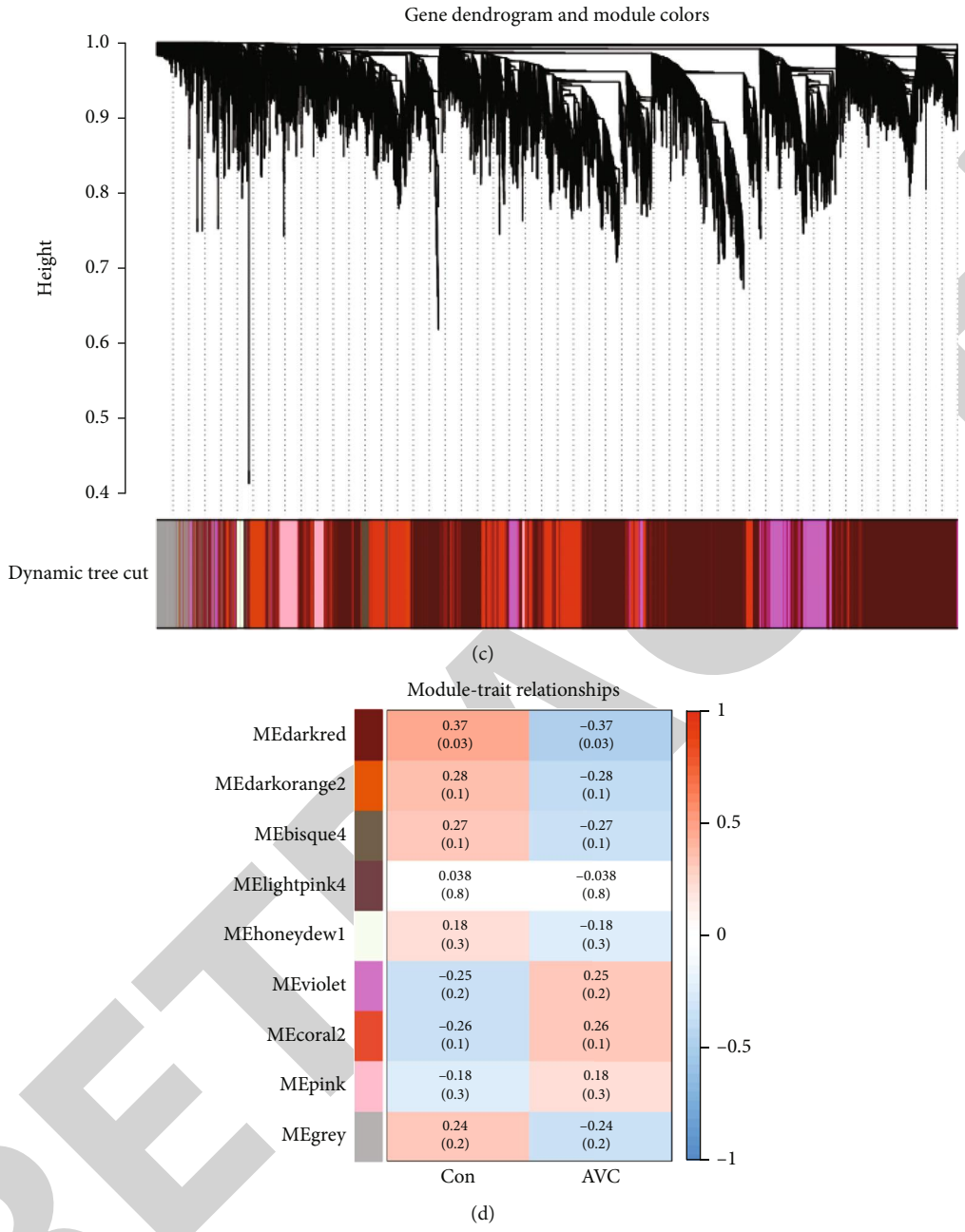

Figure 1: Differentially expressed gene analysis and weighted gene coexpression analysis of GSE12644 and GSE51472 datasets. Heatmap of differential expression analysis of GSE12644 and GSE51472 (a); cluster of weighted gene coexpression samples of GSE12644 and GSE51472 (b); gene clustering dendrogram (c); the correlation between gene modules and clinical features heatmap (d).

normalized. The differential expression analysis (Figure 1(a)) and WGCNA (Figures 1(b)–1(d)) were performed on the merged datasets. The results revealed 2416 DEGs, of which 932 genes were downregulated genes and 1484 genes were upregulated genes (Figure 1(a)). WGCNA revealed that a total of nine coexpression modules were identified. A significant negative association was found between the dark red module and AVC ($r = -0.37$, $P = 0.03$) (Figure 1(d)), which contained 11,579 genes.

3.2. Differentially Coexpressed Gene Selection. Figure 2(a) shows the Venn diagram of DEGs with genes within the dark red module, containing 1473 differentially coexpressed genes. GO (Figure 2(b)) and KEGG (Figure 2(c)) pathway enrichment analyses were conducted using differentially coexpressed genes. The pathways enriched by KEGG pathway enrichment analysis were cytokine-cytokine receptor interaction, neuroactive ligand-receptor interaction, and PI3K-Akt signaling pathway. The processes mainly enriched by GO enrichment analysis for biological process (BP) term were fatty acid metabolic process and several fatty acid-related BPs. Therefore, we focused on fatty acid metabolism-related genes for subsequent analysis. A series of 309 fatty acid metabolism-related genes were acquired by combining and deleting the duplicate

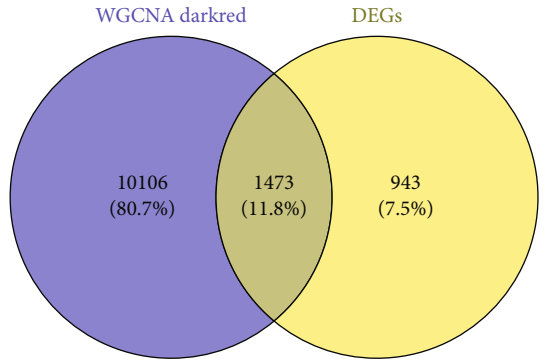

(a)

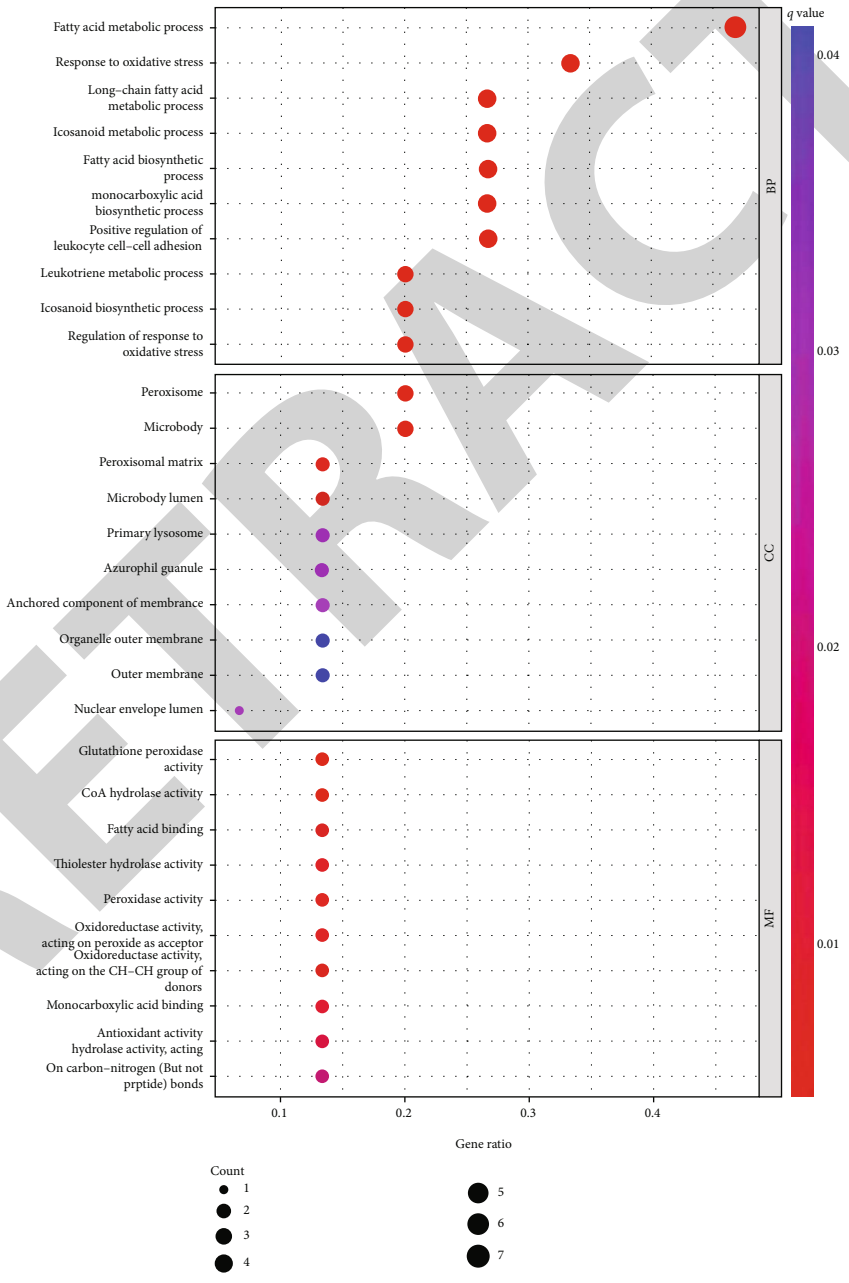

(b)

Figure 2: Continued.

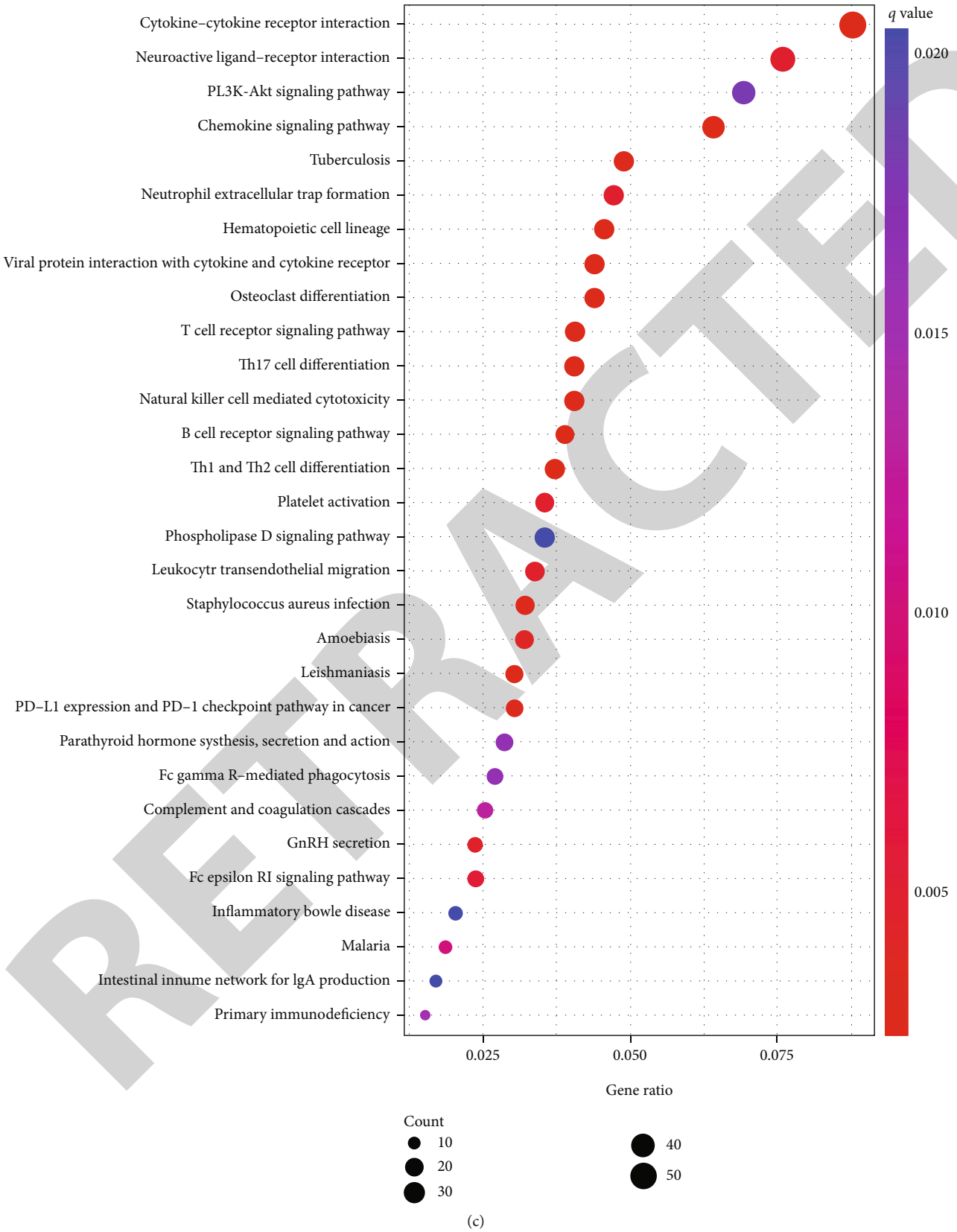

(c)

Figure 2: Continued.

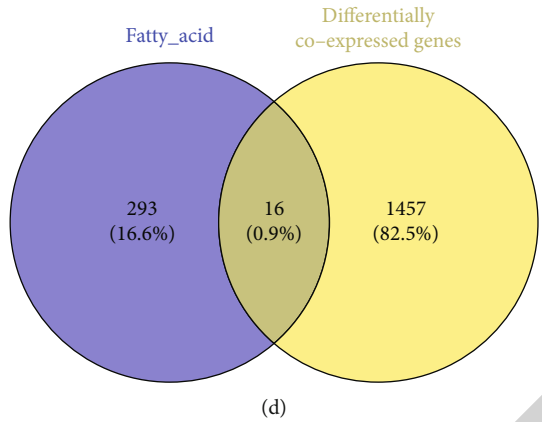

Figure 2: Detection and enrichment of differentially coexpressed genes. Venn of differentially coexpressed genes using DEGs with genes within the most significant module of WGCNA (a); GO enrichment analysis of differentially coexpressed genes (b); KEGG enrichment analysis of differentially coexpressed genes (c); fatty acid metabolism-related genes among differentially coexpressed genes by Venn diagram (d).

Table 2: Differentially coexpressed genes.

Gene symbol	logFC (fold change)	*P* value	Expression (compared to normal sample)
ACOX1	-4.41	0.019	Downregulation
ACSL4	6.75	0.041	Upregulation
CD1D	7.06	0.004	Upregulation
ERP29	65.02	0.031	Upregulation
FABP2	2.18	0.031	Upregulation
HIBCH	-73.11	0.008	Downregulation
IL4I1	14.50	0.016	Upregulation
LTC4S	-44.97	0.033	Downregulation
PRDX6	-107.19	0.022	Downregulation
VNN1	15.19	0.049	Upregulation
ACOT6	1.40	0.018	Upregulation
ACOX2	-24.82	0.039	Downregulation
ALOX5	50.67	0.034	Upregulation
DPEP1	6.46	0.004	Upregulation
PRKAA2	-5.84	0.044	Downregulation
TBXAS1	16.42	0.015	Upregulation

genes of HALLMARK_FATTY_ACID_METABOLISM, KEGG_FATTY_ACID_METABOLISM, and REACTOME_FATTY_ACID_METABOLISM from MSigDB database. A Venn diagram was plotted for the fatty acid metabolism-related genes with differentially coexpressed genes. The results revealed that 16 fatty acid metabolism-related differentially coexpressed genes were *ACOX1*, *ACSL4*, *CD1D*, *ERP29*, *FABP2*, *HIBCH*, *IL4I1*, *LTC4S*, *PRDX6*, *VNN1*, *ACOT6*, *ACOX2*, *ALOX5*, *DPEP1*, *PRKAA2*, and *TBXAS1* (Figure 2(d) and Table 2).

3.3. Detection of Fatty Acid Metabolism-Related Biomarker. LASSO regression analysis identified three genes (*ERP29*, *HIBCH*, and *PRKAA2*) from fatty acid metabolism-related differentially coexpressed genes as prospective biomarkers in AVC (Figure 3(a)). Four genes (*HIBCH*, *PRDX6*, *PRKAA2*, and *ALOX5*) were identified from fatty acid metabolism-related differentially coexpressed genes as prospective biomarkers using SVM-RFE (Figure 3(b)). Random forest selection identified one potential biomarker, 3-hydroxyisobutyryl-CoA hydrolase (HIBCH), from fatty acid metabolism-related differentially coexpressed genes (Figures 3(c) and 3(d)). To improve the accuracy of biomarkers selection and identify the AVC-related biomarker (HIBCH), the results obtained from LASSO, SVM-RFE, and random forest were merged using a Venn diagram (Figure 3(e)). The results showed that the diagnostic efficiency of HIBCH was 0.827 for the merged dataset of GSE12644 and GSE51472 (Figure 3(f)).

GSE83453 (Figures 4(a) and 4(c)) and GSE153555 (Figures 4(b) and 4(d)) datasets were used as test group. A

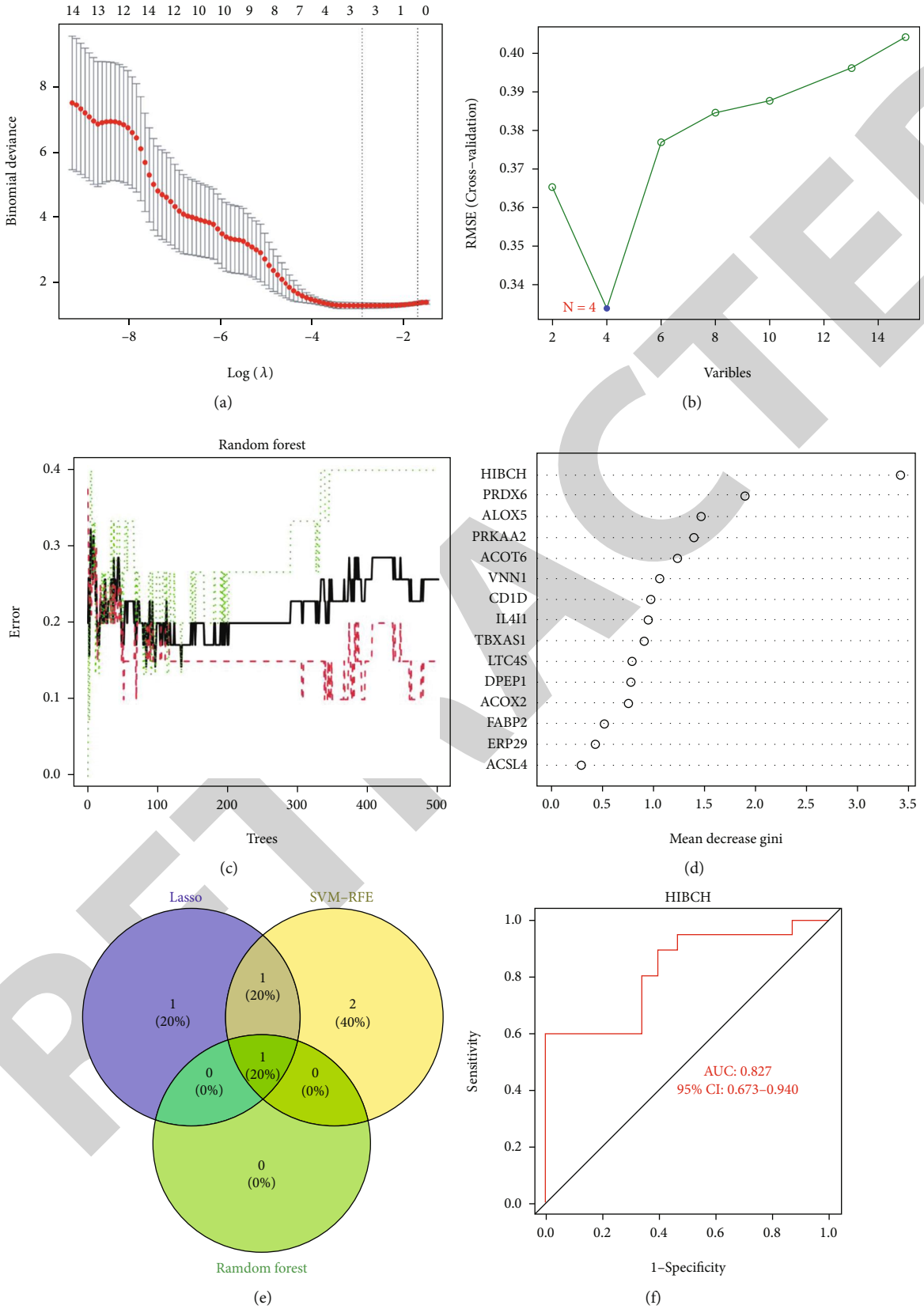

Figure 3: Detection of fatty acid metabolism-related biomarkers for AVC. Biomarker detection using LASSO regression analysis (a); biomarker detection by SVM-REF (b); biomarker detection by random forest (c and d); diagnostic markers common between LASSO, SVM-RFE, and random forest demonstrated by Venn (e); validation of HIBCH expression using ROC to access diagnostic performance of AVC (f).

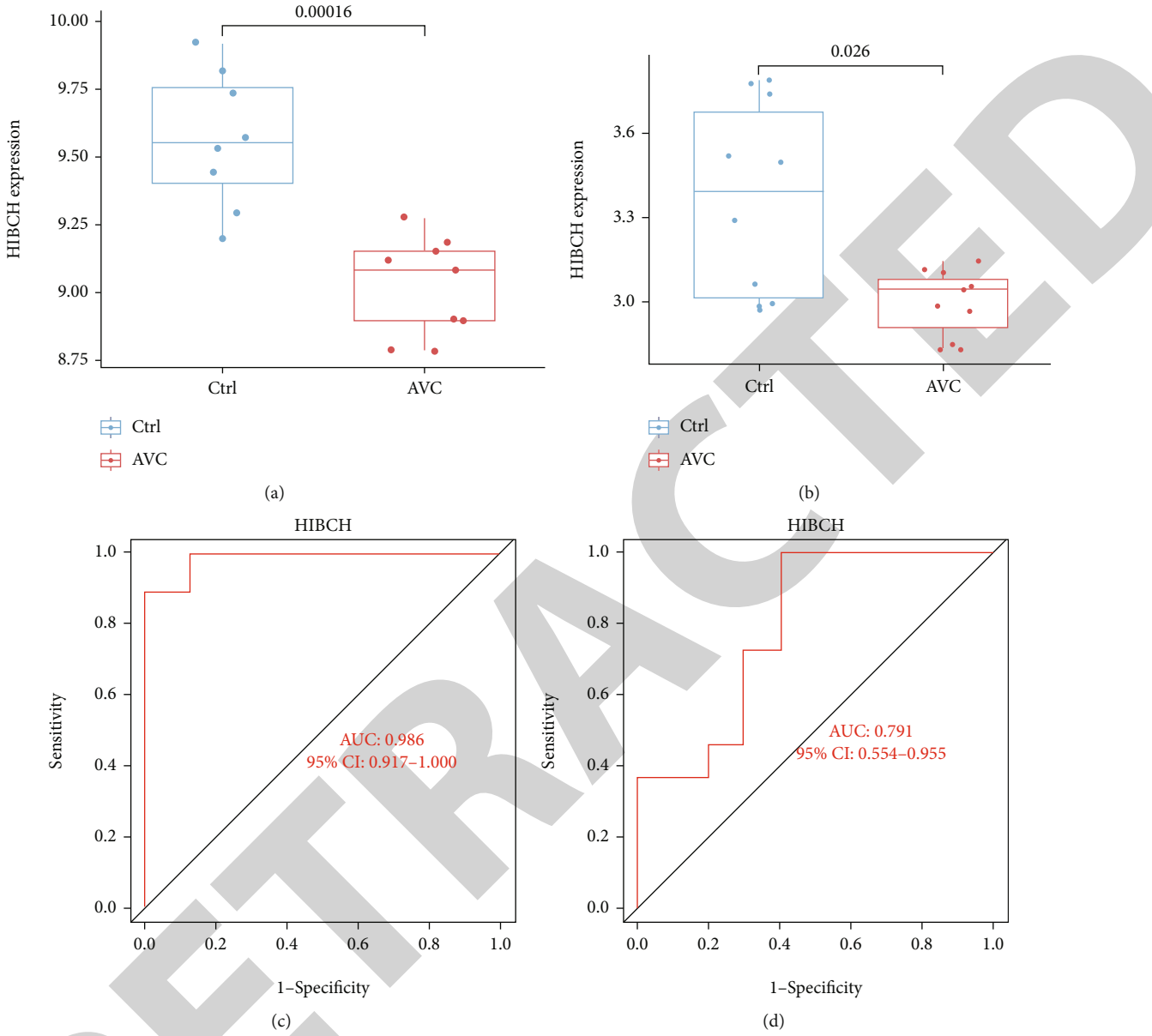

Figure 4: Validation of the diagnostic value of HIBCH. Box plot of HIBCH expression in GSE83453 (a) and ROC (c) and box plot of HIBCH expression in GSE153555 (b) and ROC (d).

remarkable decrease in HIBCH expression was noted in both GSE83453 and GSE153555 datasets. Further, both datasets had good diagnostic efficiency (AUC = 0.986 for GSE83453 and AUC = 0.791 for GSE153555). This indicates that HIBCH has a high diagnostic value.

3.4. Immune Cell Infiltration Analysis. CIBERSORT was performed to identify differences in immune infiltration between normal and AVC samples from the merged dataset (GSE12644 and GSE51472; Figures 5(a) and 5(b)). This result demonstrated that among the infiltration of twenty-two immune cells, significantly high levels of memory B cells were observed in AVC samples than normal samples ($P = 0.005$). A significantly low level of activated natural killer (NK) cells was observed in AVC than normal samples ($P = 0.024$). The relevance between twenty-two types of immune cells was investigated (Figure 5(c)). The results displayed that regulatory T cells (Tregs) were positively related to naïve B cells ($r = 0.75$). A negative correlation was observed between the activated NK cells ($r = 0.63$), M2 macrophages ($r = -0.65$), and neutrophils ($r = -0.6$). Further, activated NK cells positively correlated with activated dendritic cells ($r = 0.74$) and negatively related with M0 macrophages ($r = 0.64$) and neutrophils ($r = -0.65$). A negative relevance was found between the activated dendritic cells and M1 macrophages ($r = -0.52$). Eosinophils were positively related to naïve B cells ($r = 0.66$) and resting NK cells ($r = 0.79$). Further, eosinophils were negatively related to M2 macrophages, etc. Monocytes were negatively related to resting memory CD4 T cells ($r = 0.84$), resting NK cells ($r = 0.81$), M0 macrophages ($r = -0.78$), and plasma cells ($r = 0.67$). The resting memory CD4 T cells were positively

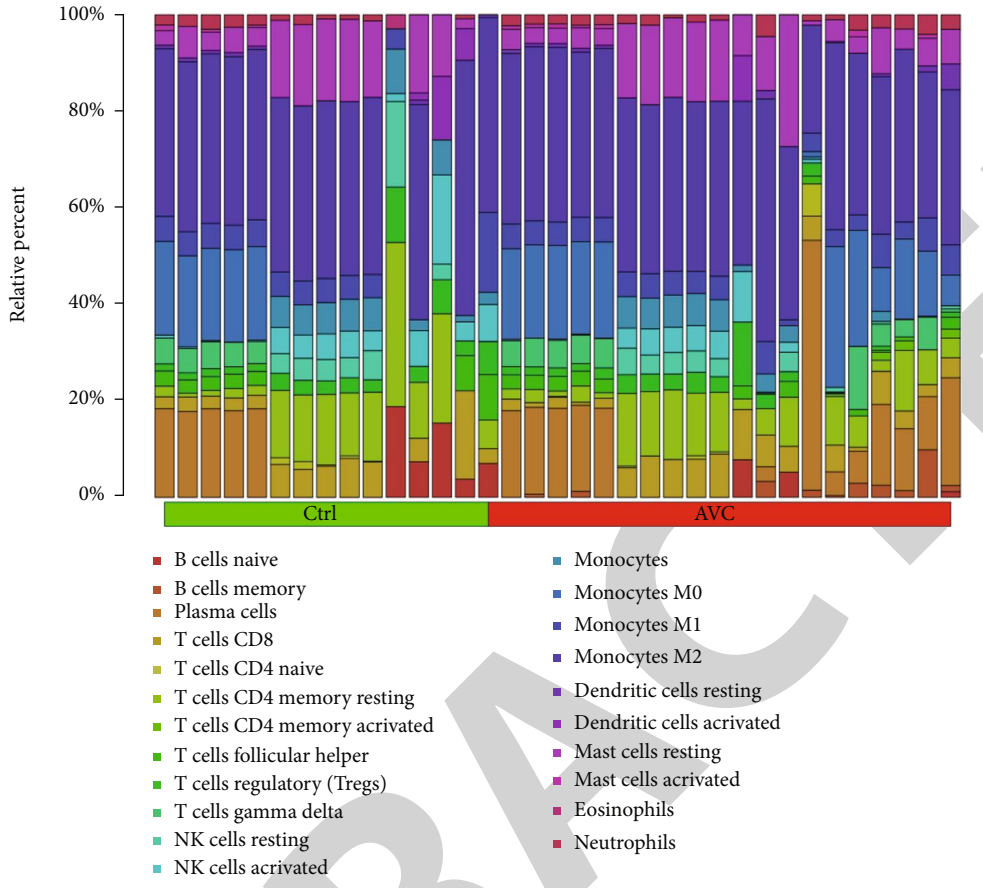

(a)

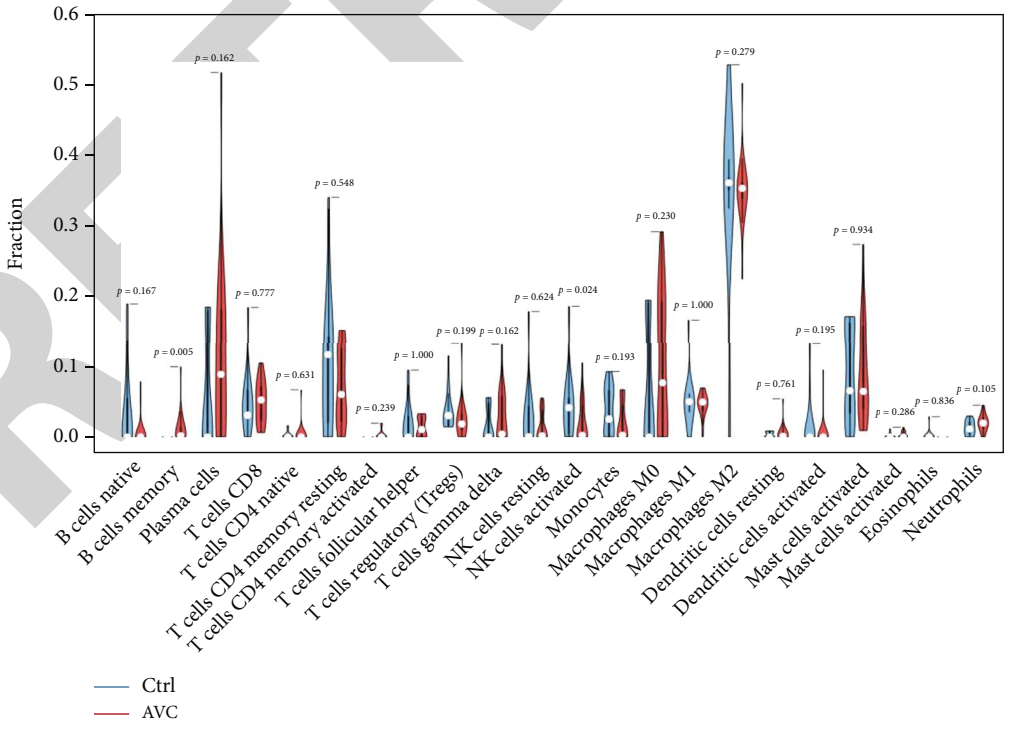

(b)

Figure 5: Continued.

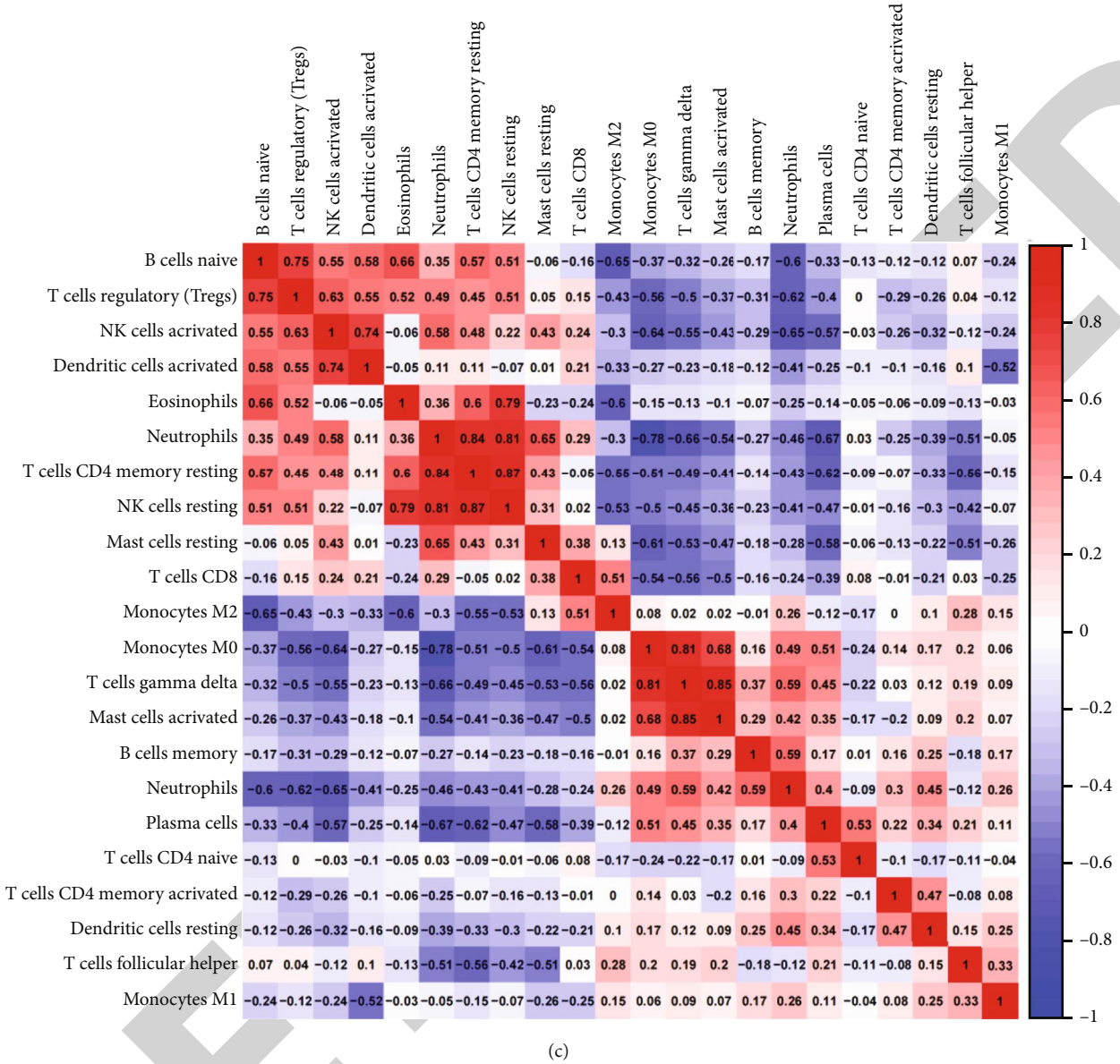

(c)

Figure 5: Immune cell content of GSE12644 and GSE51472 datasets. Immune cell content bar graph (a) and violin plot (b) and immune cell correlation heatmap (c).

related to resting NK cells ($r = 0.87$) and negatively correlated with plasma cells ($r = -0.62$) and follicular helper T cells ($r = -0.56$). The resting mast cells were positively related to resting mast cells ($r = 0.65$). The resting mast cells were negatively related to M0 macrophages ($r = -0.61$). A negative relevance was found between M2 macrophages and naive B cells ($r = -0.65$). M0 macrophages are in positive correlation with gamma delta T cells ($r = 0.81$) and activated mast cells ($r = 0.68$). Gamma delta T cell was negatively related to monocytes ($r = -0.66$) and positively related to activated mast cell ($r = 0.85$). Plasma cells were found to be positively associated with naïve CD4 T cells ($r = 0.53$) and negatively correlated with activated NK cells ($r = -0.57$). A negative relevance was observed between follicular helper T cells, monocytes ($r = -0.51$), and resting mast cells ($r = -0.51$).

3.5. HIBCH and Immune Cell Infiltration. The association between HIBCH and immunocytes was analyzed (Figure 6). The results showed significant positive relationship between HIBCH and activated NK cells ($r = 0.89$, $P = 6.2e-13$; Figure 7(a)), Tregs cells ($r = 0.86$, $P = 2.1e-11$; Figure 7(b)), monocytes ($r = 0.72$, $P = 1.3e-06$; Figure 7(c)), naive B cells ($r = 0.52$, $P = 0.0013$; Figure 7(d)), activated dendritic cells ($r = 0.51$, $P = 0.0018$; Figure 7(e)), resting memory CD4 T cells ($r = 0.44$, $P = 0.0085$; Figure 7(f)), resting NK cells ($r = 0.39$, $P = 0.022$; Figure 7(g)), and CD8 T cells ($r = 0.36$, $P = 0.033$; Figure 7(h)). A significant negative correlation was observed between HIBCH and resting dendritic cells ($r = -0.46$, $P = 0.006$; Figure 7(i)), activated mast cells ($r = -0.47$, $P = 0.0044$; Figure 7(j)), activated memory CD4 T cells ($r = -0.55$, $P = 0.00064$; Figure 7(k)), memory B cells

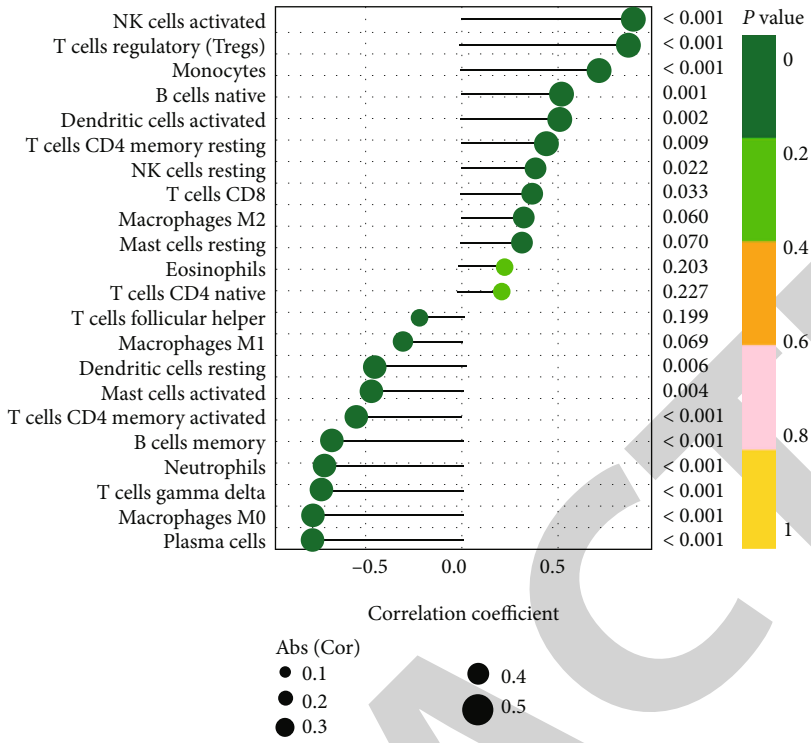

Figure 6: Correlation analysis between HIBCH and 22 immune cells.

($r = -0.68$, $P = 6.4e-06$; Figure 7(l)), neutrophils ($r = -0.72$, $P = 1.2e-06$; Figure 7(m)), gamma delta T cells ($r = -0.73$, $P = 5.8e-07$; Figure 7(n)), M0 macrophages ($r = -0.78$, $P = 3.5e-08$; Figure 7(o)), and plasma cells ($r = -0.79$, $P = 2.3e-08$; Figure 7(p)).

3.6. Single-Gene GSEA of HIBCH. Because the role of HIBCH in AVC is not clear, we predicted the potential pathways of HIBCH using single-gene GSEA. Interestingly, the results of single-gene GSEA once again suggest that HIBCH is closely associated with immunity. B_CELL_RECEPTOR_SIGNALING_PATHWAY (NES = −1.56, $P = 0.028$), CHEMOKINE_SIGNALING_PATHWAY (NES = −1.47, $P = 0.041$), and INTESTINAL_IMMUNE_NETWORK_FOR_IGA_PRODUCTION (NES = −1.47, $P = 0.041$) are enriched in the low-expressing HIBCH group. This indicates that HIBCH may act by inhibiting these immune-related pathways (Figure 8).

4. Discussion

AVC is a commonly occurring valvular disease globally. AVC is characterized by progressive fibrosis and calcification of the aortic valve and is asymptomatic for a prolonged period. Surgical treatment is required in patients with serious symptoms and has a poor prognosis [19]. The pathogenesis of AVC is complex and similar to atherosclerosis, involving multiple pathological processes including chronic inflammation, lipid metabolism disorders, fibrosis, and calcification [20]. This is consistent with our analysis using publicly available databases and bioinformatic analysis that AVC may be closely associated with fatty acid metabolism. Previous investigations show that although lipids are primarily associated with AVC pathogenesis, statins have no significant benefits in improving aortic stenosis according to the literature [21–23]. Therefore, identifying and developing effective treatments and therapeutic strategies for AVC is an important area of research in cardiac diseases.

In our research, differentially coexpressed genes in AVC were evaluated using DEG and WGCNA, followed by GO and KEGG pathway enrichment analyses. The consequences found that AVC might be strongly associated with fatty acid metabolism. We then obtained fatty acid metabolism-related genes through MsigDB database. LASSO regression analysis, SVM-REF, and random forest identified HIBCH as a fatty acid metabolism-related biomarker for AVC. Further, two datasets were used for external validation, and the results revealed good predictive performance by both, indicating that HIBCH has a high diagnostic value. As of right now, in regard to the link between fatty acid metabolism and AVC, numerous studies point to the possibility that PCSK9 is essential for Lp(a) catabolism, which has a significant effect on the development of AVC [24–26]. The multiple machine learning combined in this study further uncovered the relationship between important genes associated with fatty acid metabolism and AVC, which might provide new perspectives for subsequent studies. Finally, the differences in immune cell levels between AVC and normal samples and the pertinence between HIBCH and twenty-two immune cells were analyzed. The results showed a significant association between HIBCH and various immune cells. This suggests that HIBCH in AVC tissues might impact the

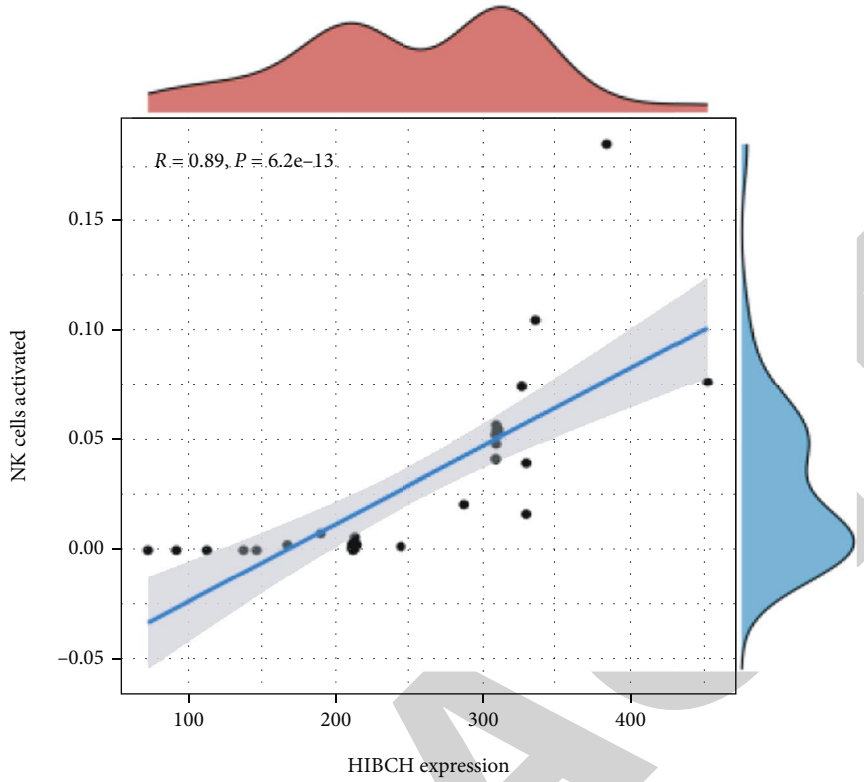

(a)

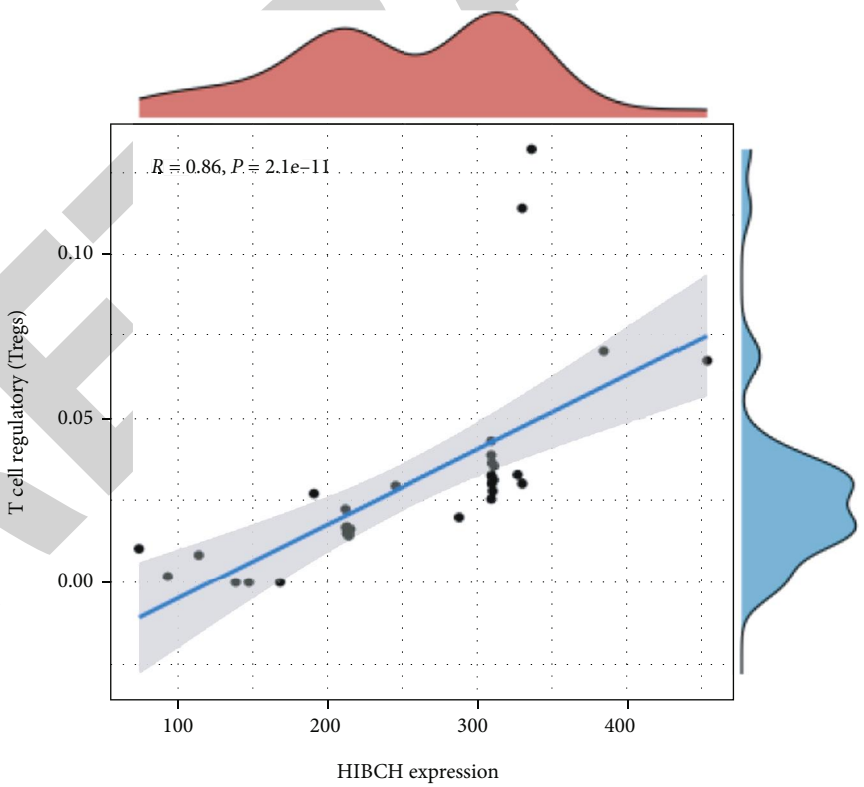

(b)

Figure 7: Continued.

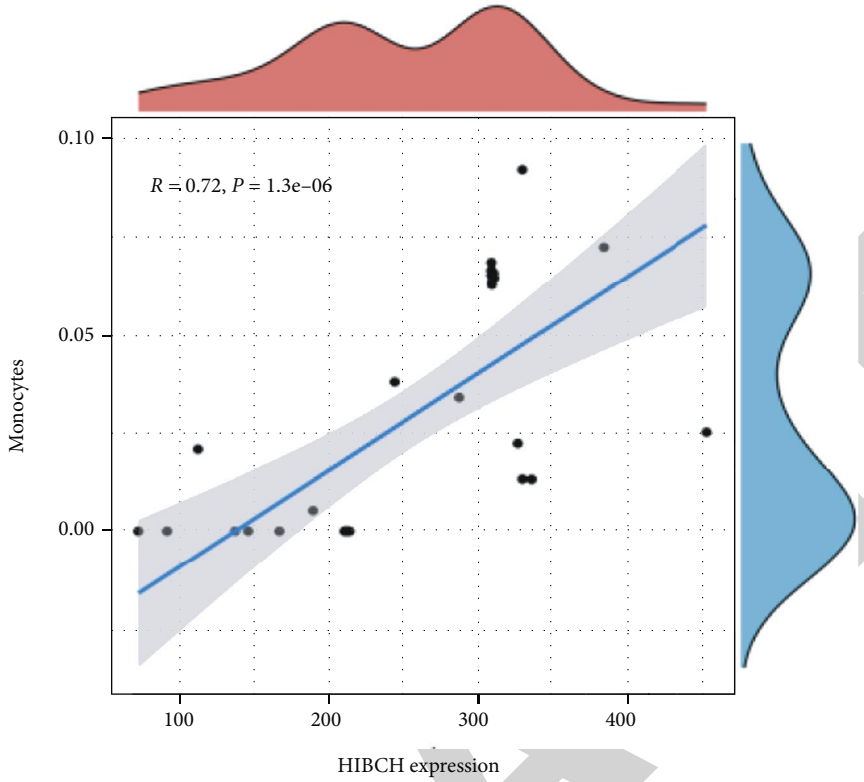

(c)

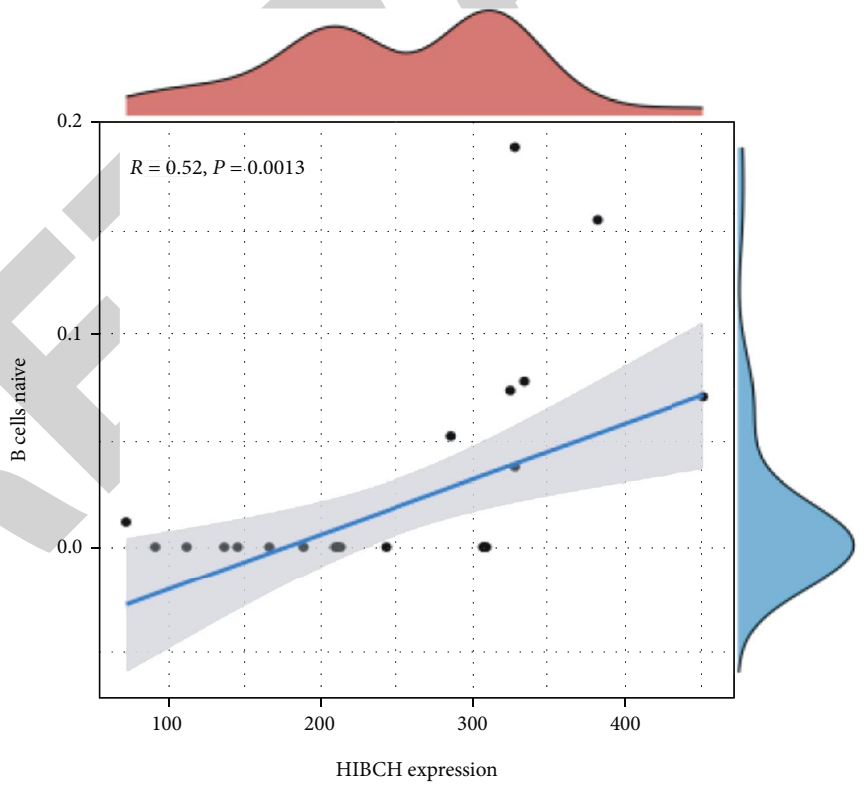

(d)

Figure 7: Continued.

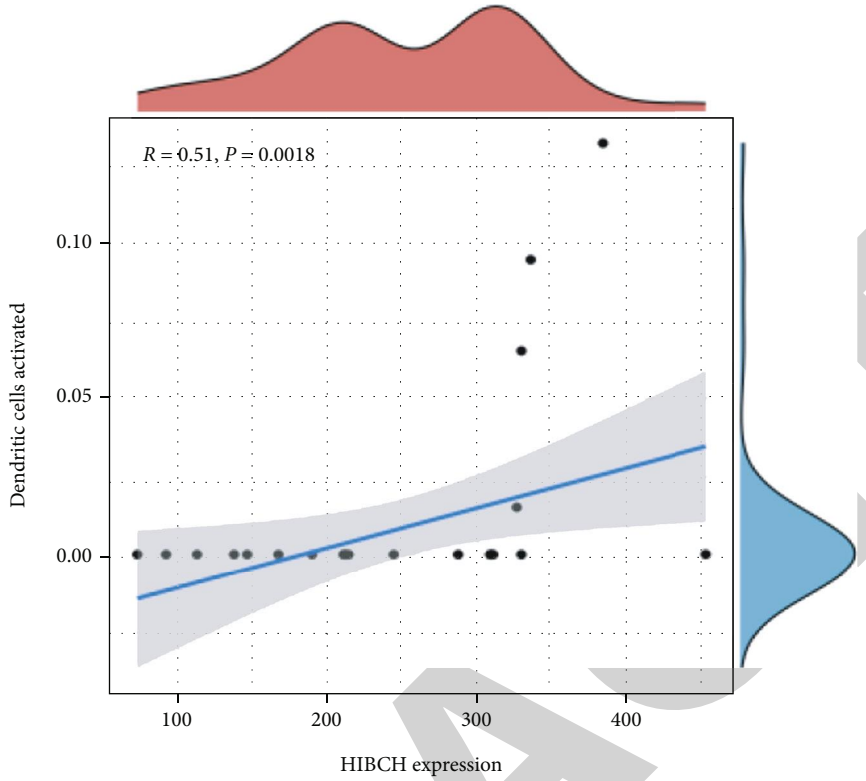

(e)

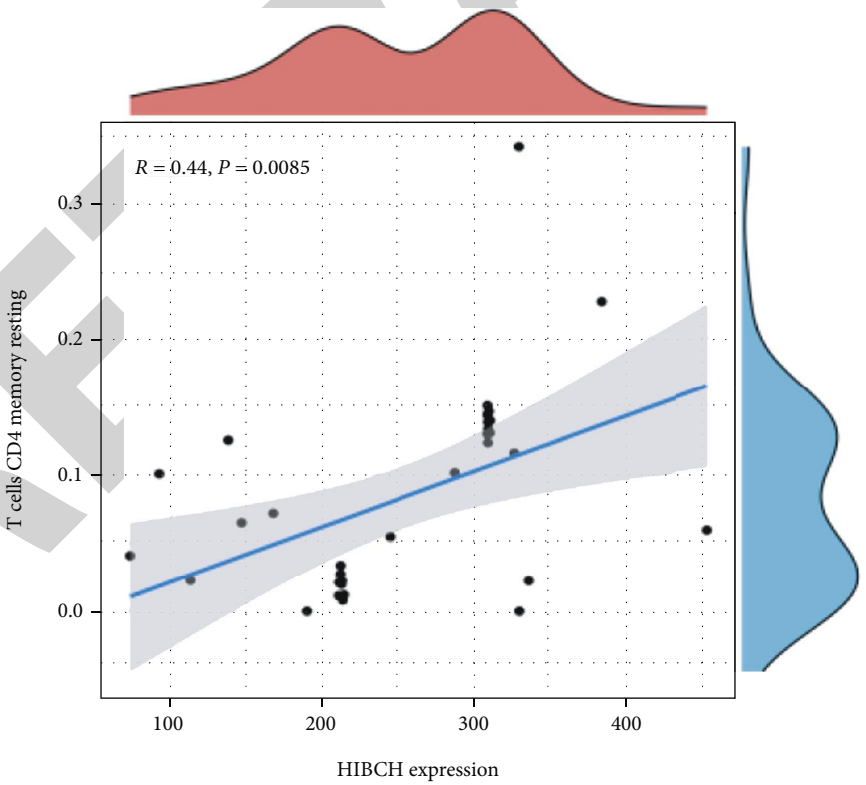

(f)

Figure 7: Continued.

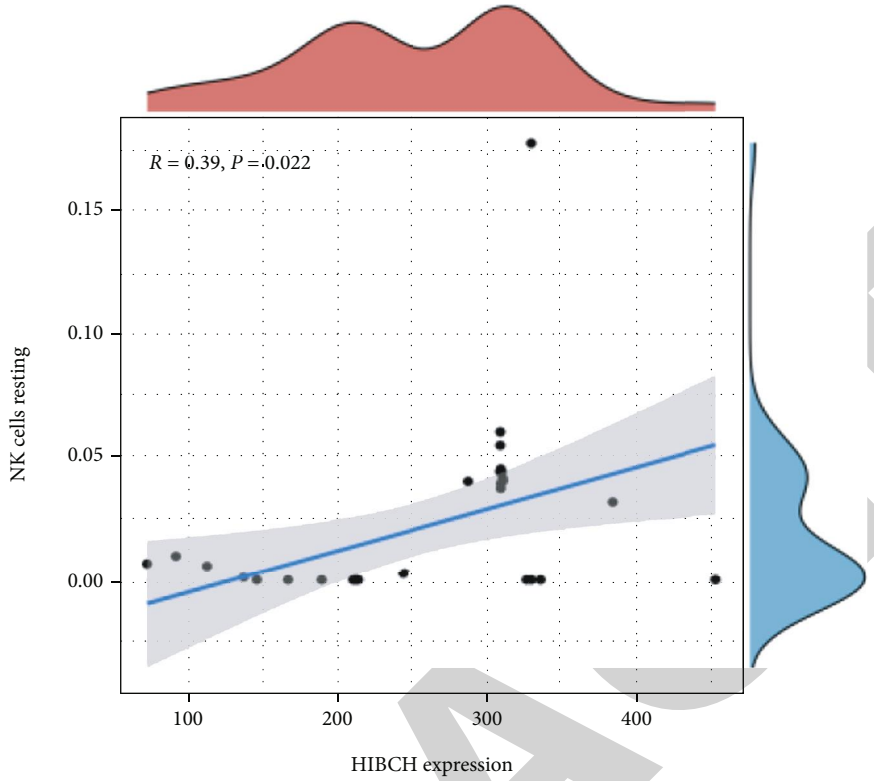

(g)

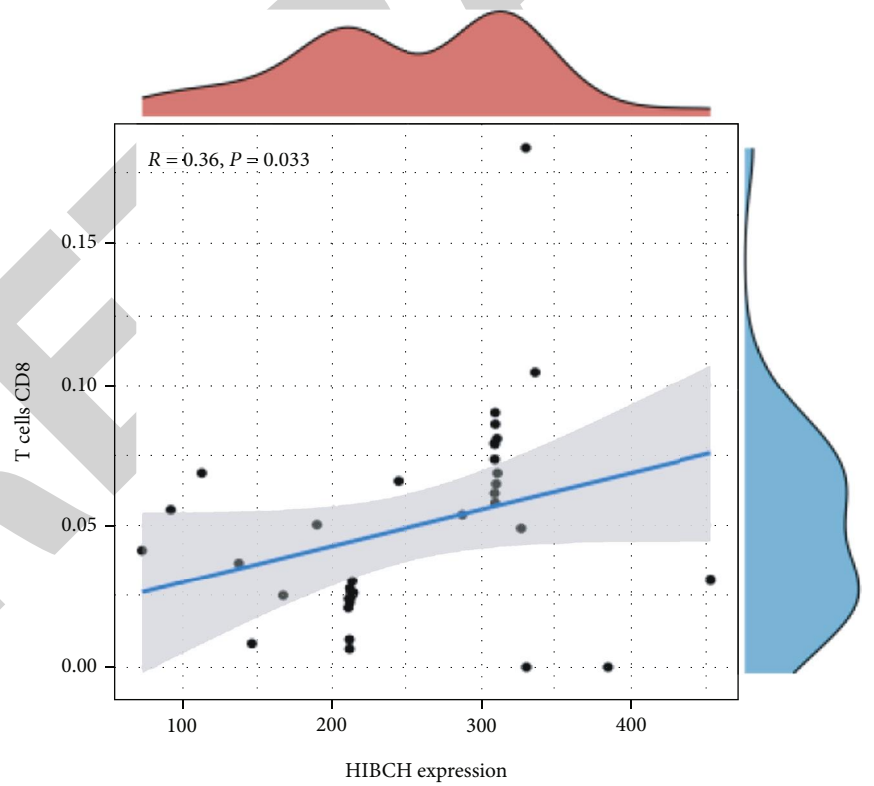

(h)

Figure 7: Continued.

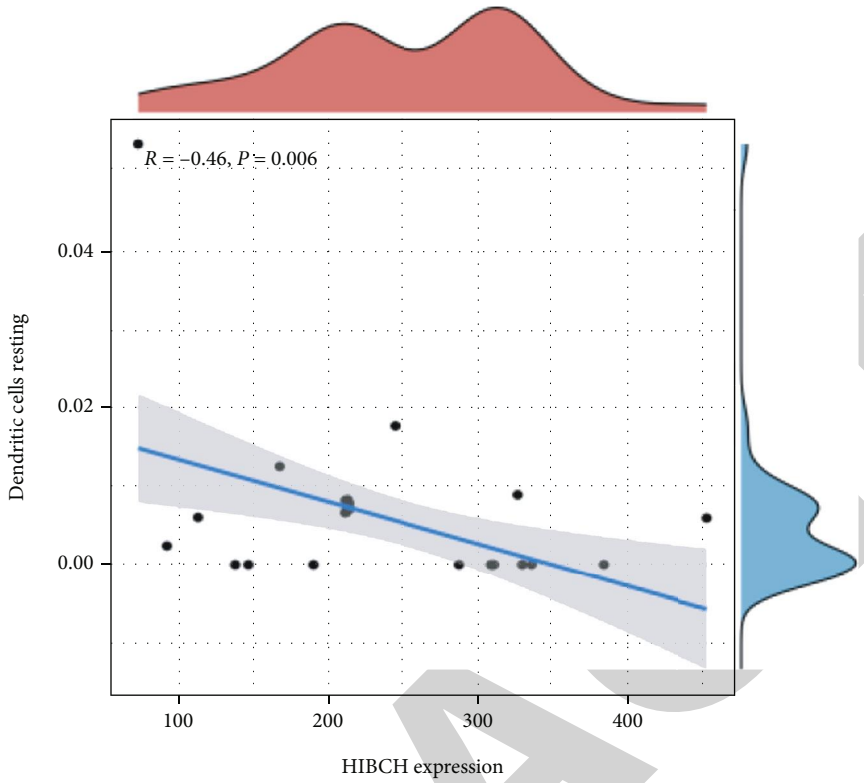

(i)

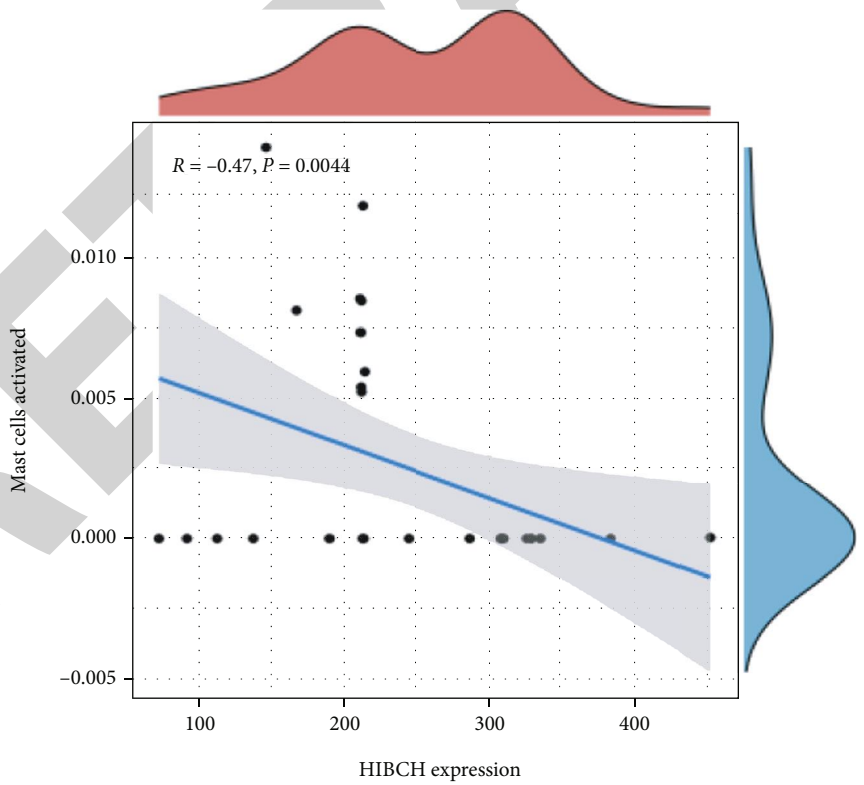

(j)

Figure 7: Continued.

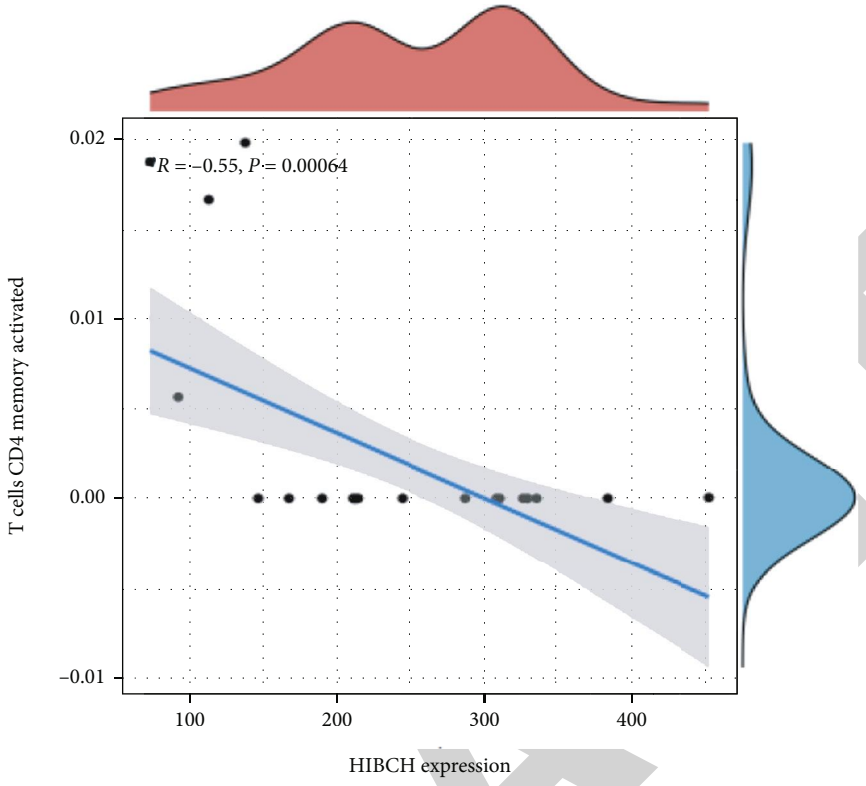

(k)

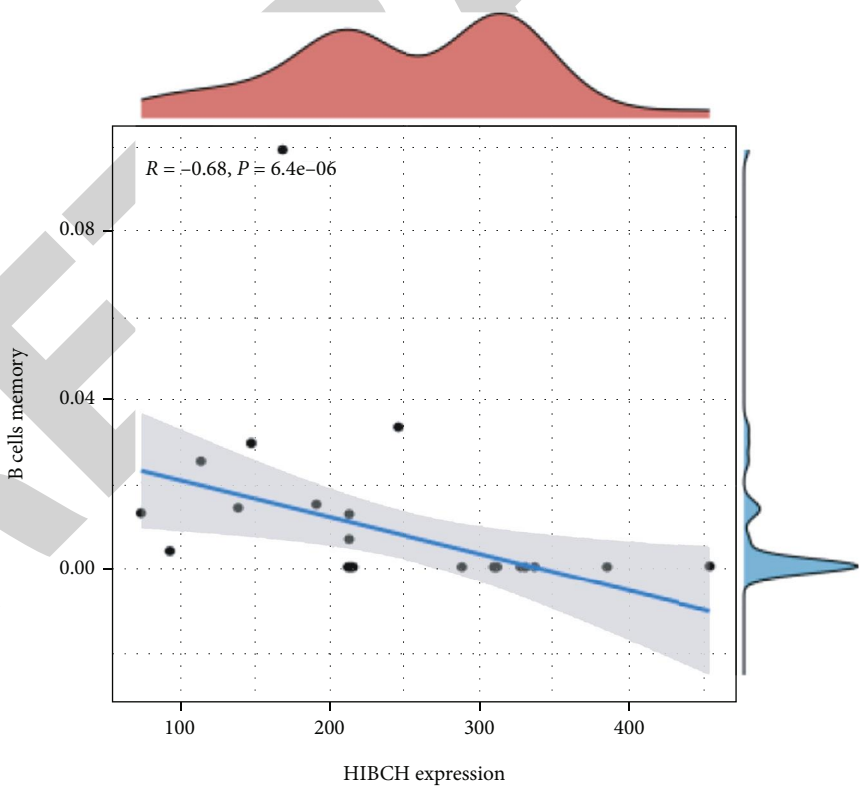

(l)

Figure 7: Continued.

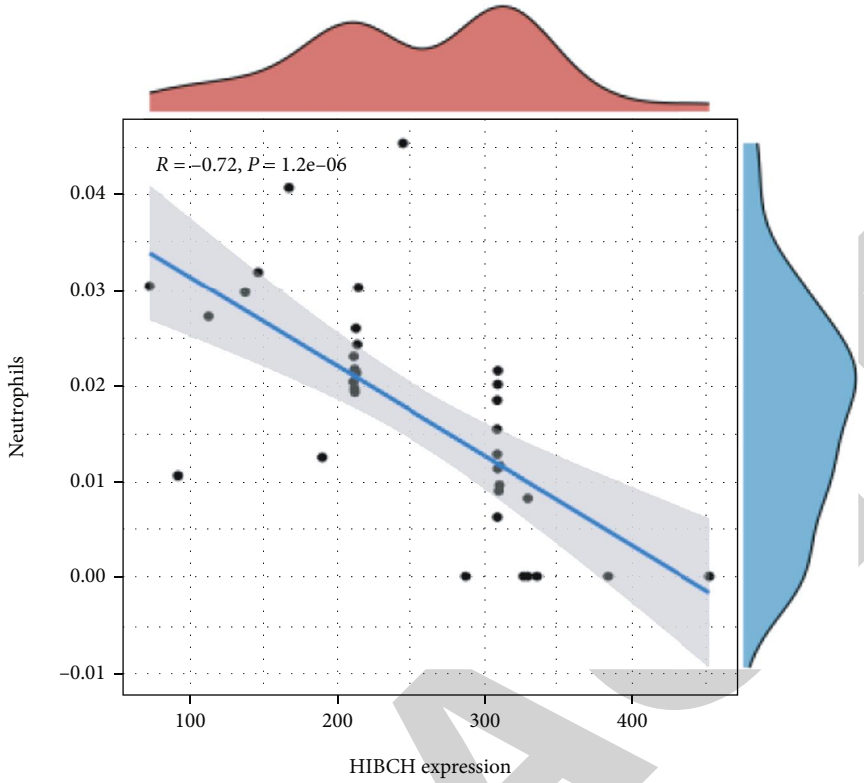

(m)

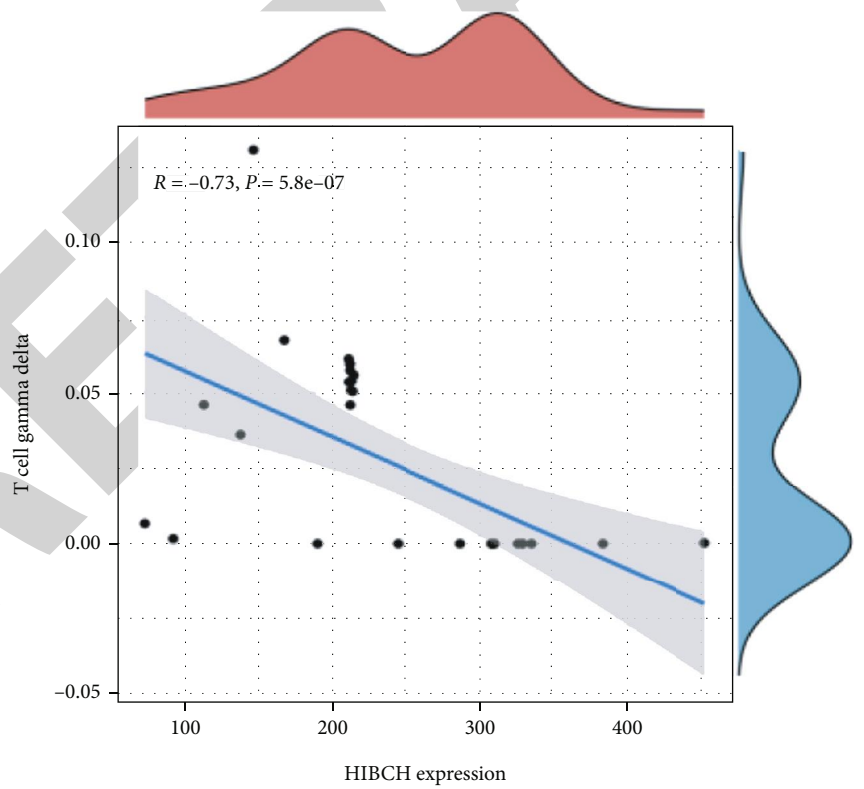

(n)

Figure 7: Continued.

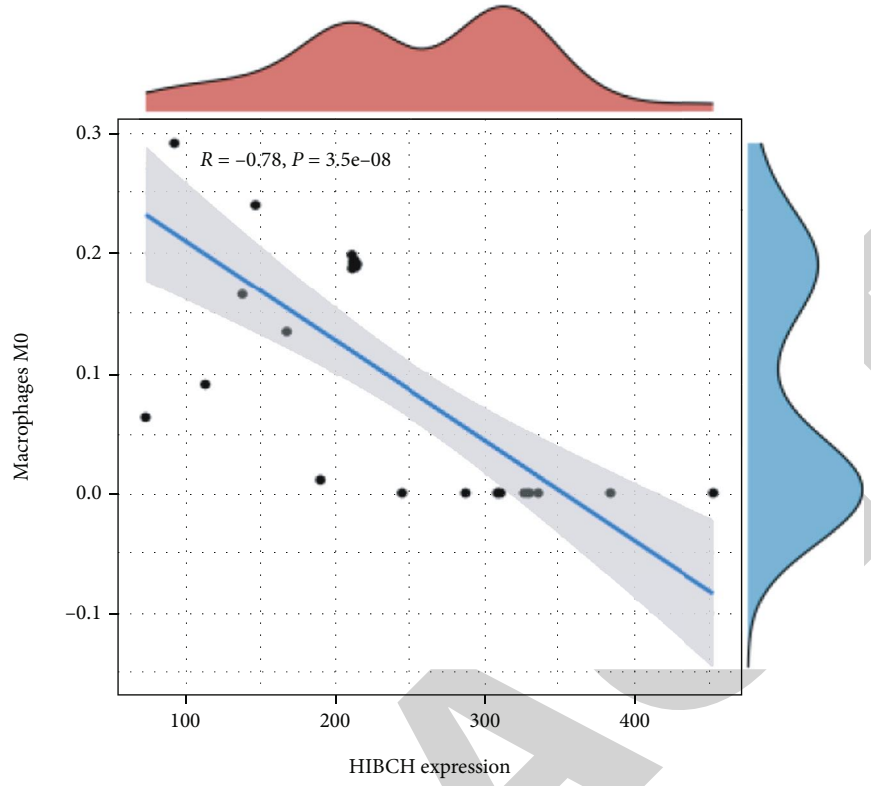

(o)

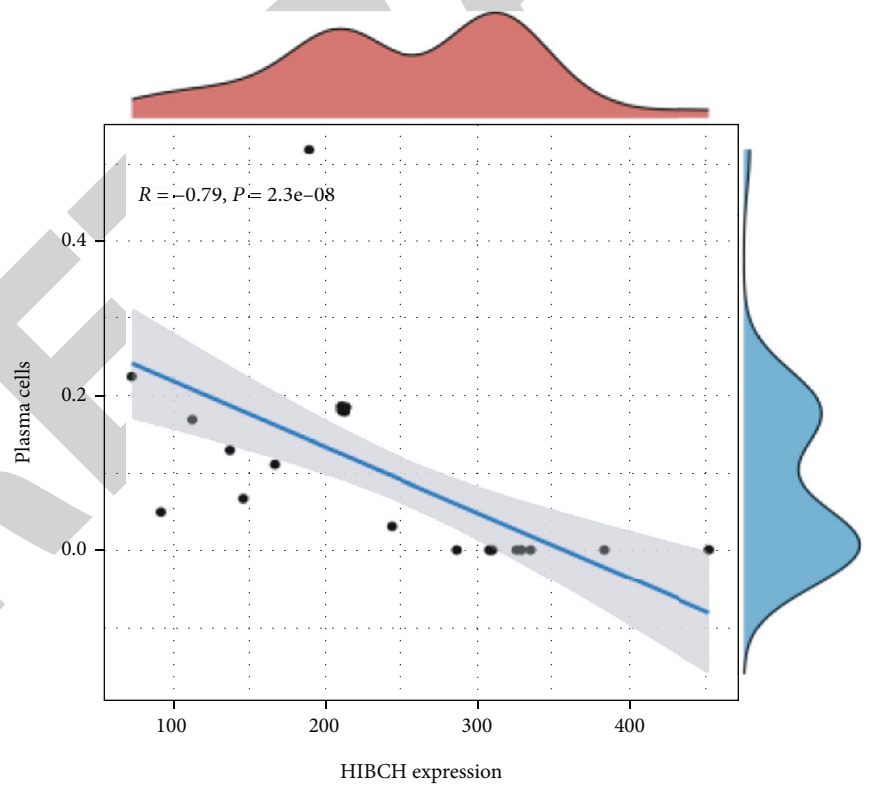

(p)

Figure 7: Graph of HIBCH correlation with 22 immune cell types. Correlation analysis of HIBCH and activated NK cells (a), regulatory T cells (b), monocytes (c), naïve B cells (d), activated dendritic cells (e), resting memory CD4 T cells (f), resting NK cells (g), CD8 T cells (h), resting dendritic cells (i), activated mast cells (j), activated memory CD4 T cells (k), memory B cells (l), Neutrophils (m), gamma delta T cells (n), M0 macrophages (o), and Plasma cells (p).

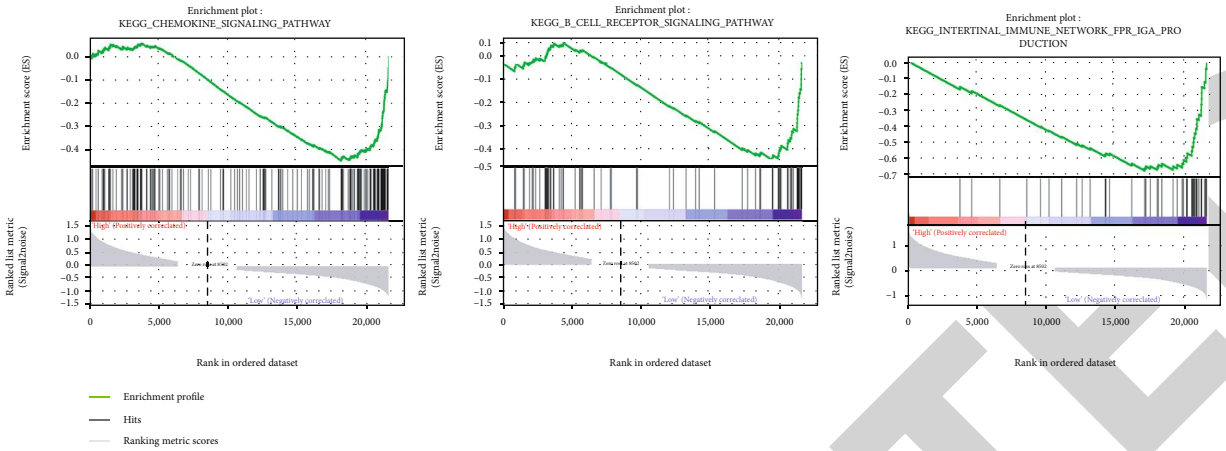

Figure 8: Single-gene GSEA of HIBCH.

progression of AVC by affecting immune cells. The GSEA results provide additional evidence that HIBCH may act through immune-related pathways.

HIBCH (3-hydroxyisobutyryl-CoA hydrolase) is an enzyme that catalyzes the conversion of 3-hydroxyisobutyryl-CoA to 3-hydroxyisobutyric acid [27]. It is a key mitochondrial protein required for valine catabolism [28, 29]. The metabolite 3-hydroxyisobutyric acid is transformed further to succinyl coenzyme A which is involved in the metabolism of the tricarboxylic acid (TCA) cycle. A prior research has reported the involvement of HIBCH in hepatic mitochondrial fatty acid oxidation [30]. Various studies have shown that HIBCH is related to colorectal cancer [31], ovarian cancer [32, 33], prostate cancer [34], paroxysmal dyskinesia [35], and Leigh syndrome [36–39]. In addition, a study also showed the association between HIBCH with AVC [40].

With the advancement in the understanding of AVC, various researches have demonstrated the effect of immune cells in AVC. Previous studies have shown that both antigen-presenting cells (APCs) and macrophages exist in normal and pathologic valves, but the existence of T lymphocytes is characteristic of both aging and pathologic valves [41, 42]. This lymphocytic infiltration is accompanied by increased neointima formation and osteogenesis, which is the hallmark and pathological signs of AVC [43]. The abundance of B lymphocytes in the valves is related to increased disease severity. In addition, prior researches showed that the depletion of natural killer T (NKT) cells can lead to improvement or worsening of a variety of fibrotic diseases [44–46]. Nevertheless, the effects of B lymphocytes and NKT cells in AVC are not clear. CIBERSORT analysis revealed significantly high levels of memory B cells in AVC than normal samples. The levels of activated NK cells were significantly low in AVC samples compared to normal samples. A clear inverse correlation between HIBCH and memory B cells and a positive relationship between HIBCH and activated NK cells were observed in AVC. This suggests that high expression of HIBCH may be able to promote the infiltration of activated NK cells and inhibit the infiltration of memory B cells.

The GSEA results suggest that HIBCH may be closely associated with chemokine signaling pathways in AVC patients. Although there are no reports on the interregulatory relationship between HIBCH and chemokines, a previous study examined genome-wide gene expression profiles at different stages of AVC and found that the most significant changes were in inflammatory and immune-related genes containing chemokines CCL3 and CCL4. This study verified that CCL3 and CCL4 expressions were increased in AVC and was predominantly localized in macrophage-rich environments [47]. In addition, several chemokines, CCL18 [48] and CCL23 [49], have been associated with atherosclerosis. Similar to our results, several recent bioinformatic articles have reported that chemokine-related pathways and chemokines may play an important role in AVC [50, 51]. In a study of the association between AVC and systemic lupus erythematosus (SLE) prognosis, Molad et al. reported that AVC and mitral annular calcification (MAC) were significantly and positively associated with serum IgA isotype of anticardiolipin antibody [52]. Our study found a decrease of HIBCH expression in AVC patients, and GSEA suggests that low expression of HIBCH may be associated with IgA production. However, the role of chemokines and IgA in AVC still needs to be further investigated. Similarly, the relationship between HIBCH and chemokines and IgA production still needs to be explored more.

Investigations into potential treatments for calcification of the aortic valve are continuously ongoing. As a particular inhibitor of hydroxymethylglutaryl-coenzyme A reductase, statins are applied to cure a broad variety of diseases, including inflammation and atherosclerosis. Even while retrospective investigations showed that statins could possibly be of help in AVC, further randomized controlled trials revealed that statins really make no difference to AVC or to clinical outcomes. This result was backed up by the findings of a second meta-analysis [53]. When the disease has progressed to fibrosis and calcification, statins have very little impact. This is the most likely reason for this failure. Based on the findings presented above, it seems that the use of HIBCH inhibitors might be a prospective target of AVC.

In this research, we identified fatty acid metabolism-related biomarkers in AVC and their relationship with

immune cells. However, the small sample size of AVC-related data in publicly available databases was small. Hence, the diagnostic value of HIBCH further validation in a larger sample size of AVC patients is still needed. Additionally, the role and mechanism of HIBCH in the development of AVC and its relationship with immune cells still need further experimental validation of our findings.

5. Conclusions

In this research, we found that HIBCH is a diagnostic marker of AVC using DEG analysis, LASSO, SVM-REF, and random forest. The results were validated in external datasets. The analysis conducted using CIBERSORT revealed that HIBCH was strongly connected with immune infiltration of AVC. Finally, the possible role of HIBCH through immune-related pathways was further predicted by GSEA.

Data Availability

The data used to support the results of this study are available from the authors upon request.

Conflicts of Interest

The authors declare that there is no conflict of interest regarding the publication of this paper.

Authors' Contributions

Jun-Yu Chen and Qing Chang designed the research. Ya-Ru Sun, Tao Xiong, and Guan-Nan Wang performed the literature search as well as collected and assembled the data. Jun-Yu Chen, Ya-Ru Sun, Tao Xiong, and Guan-Nan Wang prepared the manuscript. Qing Chang revised the manuscript critically. The complete article was created under the supervision of Qing Chang.

Acknowledgments

This study was sponsored by the fund from the Qingdao West Coast New Area Science and Technology Project (No. 2020-51).

References

[1] S. Yadgir, C. O. Johnson, V. Aboyans et al., "Global, regional, and national burden of calcific aortic valve and degenerative mitral valve diseases, 1990-2017," *Circulation*, vol. 141, no. 21, pp. 1670–1680, 2020.

[2] C. M. Otto and B. Prendergast, "Aortic-valve stenosis–from patients at risk to severe valve obstruction," *New England Journal of Medicine*, vol. 371, no. 8, pp. 744–756, 2014.

[3] J. Lincoln and V. Garg, "Etiology of valvular heart disease-genetic and developmental origins," *Circulation Journal*, vol. 78, no. 8, pp. 1801–1807, 2014.

[4] B. R. Lindman, M. A. Clavel, P. Mathieu et al., "Calcific aortic stenosis," *Nature Reviews. Disease Primers*, vol. 2, no. 1, article 16006, 2016.

[5] P. R. Goody, M. R. Hosen, D. Christmann et al., "Aortic valve stenosis," *Arteriosclerosis Thrombosis and Vascular Biology*, vol. 40, no. 4, pp. 885–900, 2020.

[6] F. Peeters, S. J. R. Meex, M. R. Dweck et al., "Calcific aortic valve stenosis: hard disease in the heart," *European Heart Journal*, vol. 39, no. 28, pp. 2618–2624, 2018.

[7] D. H. Kang, S. J. Park, J. H. Rim et al., "Early surgery versus conventional treatment in asymptomatic very severe aortic stenosis," *Circulation*, vol. 121, no. 13, pp. 1502–1509, 2010.

[8] F. J. Schoen and R. J. Levy, "Calcification of tissue heart valve substitutes: progress toward understanding and prevention," *Annals of Thoracic Surgery*, vol. 79, no. 3, pp. 1072–1080, 2005.

[9] M. E. Ritchie, B. Phipson, D. Wu et al., "Limma powers differential expression analyses for RNA-sequencing and microarray studies," *Nucleic Acids Research*, vol. 43, no. 7, article e47, 2015.

[10] P. Langfelder and S. Horvath, "WGCNA: an R package for weighted correlation network analysis," *BMC Bioinformatics*, vol. 9, no. 1, p. 559, 2008.

[11] G. Yu, L. G. Wang, Y. Han, and Q. Y. He, "clusterProfiler: an R package for comparing biological themes among gene clusters," *OMICS*, vol. 16, no. 5, pp. 284–287, 2012.

[12] X. Lin, F. Yang, L. Zhou et al., "A support vector machine-recursive feature elimination feature selection method based on artificial contrast variables and mutual information," *Journal of Chromatography. B, Analytical Technologies in the Biomedical and Life Sciences*, vol. 910, pp. 149–155, 2012.

[13] F. M. Alakwaa, K. Chaudhary, and L. X. Garmire, "Deep learning accurately predicts estrogen receptor status in breast cancer metabolomics data," *Journal of Proteome Research*, vol. 17, no. 1, pp. 337–347, 2018.

[14] H. Wang, B. J. Lengerich, B. Aragam, and E. P. Xing, "Precision Lasso: accounting for correlations and linear dependencies in high-dimensional genomic data," *Bioinformatics*, vol. 35, no. 7, pp. 1181–1187, 2019.

[15] J. Friedman, T. Hastie, and R. Tibshirani, "Regularization paths for generalized linear models via coordinate descent," *Journal of Statistical Software*, vol. 33, no. 1, pp. 1–22, 2010.

[16] M. L. Huang, Y. H. Hung, W. M. Lee, R. K. Li, and B. R. Jiang, "SVM-RFE based feature selection and Taguchi parameters optimization for multiclass SVM classifier," *The Scientific World Journal*, vol. 2014, Article ID 795624, 10 pages, 2014.

[17] X. Robin, N. Turck, A. Hainard et al., "pROC: an open-source package for R and S+ to analyze and compare ROC curves," *BMC Bioinformatics*, vol. 12, no. 1, p. 77, 2011.

[18] A. M. Newman, C. L. Liu, M. R. Green et al., "Robust enumeration of cell subsets from tissue expression profiles," *Nature Methods*, vol. 12, no. 5, pp. 453–457, 2015.

[19] Y. Sasakawa, N. Okamoto, M. Fujii, J. Kato, Y. Yuzawa, and D. Inaguma, "Factors associated with aortic valve stenosis in Japanese patients with end-stage kidney disease," *BMC Nephrology*, vol. 23, no. 1, p. 129, 2022.

[20] M. J. Nsaibia, A. Devendran, E. Goubaa, J. Bouitbir, R. Capoulade, and R. Bouchareb, "Implication of lipids in calcified aortic valve pathogenesis: why did statins fail?," *Journal of Clinical Medicine*, vol. 11, no. 12, 2022.

[21] S. J. Cowell, D. E. Newby, R. J. Prescott et al., "A randomized trial of intensive lipid-lowering therapy in calcific aortic stenosis," *New England Journal of Medicine*, vol. 352, no. 23, pp. 2389–2397, 2005.

[22] A. B. Rossebø, T. R. Pedersen, K. Boman et al., "Intensive lipid lowering with simvastatin and ezetimibe in aortic stenosis," *New England Journal of Medicine*, vol. 359, no. 13, pp. 1343–1356, 2008.

[23] K. L. Chan, K. Teo, J. G. Dumesnil, A. Ni, J. Tam, and ASTRONOMER Investigators, "Effect of lipid lowering with rosuvastatin on progression of aortic stenosis: results of the aortic stenosis progression observation: measuring effects of rosuvastatin (ASTRONOMER) trial," *Circulation*, vol. 121, no. 2, pp. 306–314, 2010.

[24] W. G. Wang, Y. F. He, Y. L. Chen et al., "Proprotein convertase subtilisin/kexin type 9 levels and aortic valve calcification: a prospective, cross sectional study," *Journal of International Medical Research*, vol. 44, no. 4, pp. 865–874, 2016.

[25] M. J. Nsaibia, A. Mahmut, H. Mahjoub et al., "Association between plasma lipoprotein levels and bioprosthetic valve structural degeneration," *Heart*, vol. 102, no. 23, pp. 1915–1921, 2016.

[26] C. Goettsch, J. D. Hutcheson, S. Hagita et al., "A single injection of gain-of-function mutant PCSK9 adeno-associated virus vector induces cardiovascular calcification in mice with no genetic modification," *Atherosclerosis*, vol. 251, pp. 109–118, 2016.

[27] K. Taniguchi, T. Nonami, A. Nakao et al., "The valine catabolic pathway in human liver: effect of cirrhosis on enzyme activities," *Hepatology*, vol. 24, no. 6, pp. 1395–1398, 1996.

[28] G. Rendina and M. J. Coon, "Enzymatic hydrolysis of the coenzyme a thiol esters of beta-hydroxypropionic and beta-hydroxyisobutyric acids," *Journal of Biological Chemistry*, vol. 225, no. 1, pp. 523–534, 1957.

[29] Y. Shimomura, T. Murakami, N. Fujitsuka et al., "Purification and partial characterization of 3-hydroxyisobutyryl-coenzyme A hydrolase of rat liver," *Journal of Biological Chemistry*, vol. 269, no. 19, pp. 14248–14253, 1994.

[30] M. S. Bjune, C. Lindquist, M. H. Stafsnes et al., "Plasma 3-hydroxyisobutyrate (3-HIB) and methylmalonic acid (MMA) are markers of hepatic mitochondrial fatty acid oxidation in male Wistar rats," *Biochimica et Biophysica Acta, Molecular and Cell Biology of Lipids*, vol. 1866, no. 4, article 158887, 2021.

[31] Y. Shan, Y. Gao, W. Jin et al., "Targeting HIBCH to reprogram valine metabolism for the treatment of colorectal cancer," *Cell Death and Disease*, vol. 10, no. 8, p. 618, 2019.

[32] N. Li, N. Li, S. Wen et al., "HSP60 regulates lipid metabolism in human ovarian cancer," *Oxidative Medicine and Cellular Longevity*, vol. 2021, Article ID 6610529, 21 pages, 2021.

[33] N. Li and X. Zhan, "Signaling pathway network alterations in human ovarian cancers identified with quantitative mitochondrial proteomics," *The EPMA Journal*, vol. 10, no. 2, pp. 153–172, 2019.

[34] J. N. Graff, S. Puri, C. B. Bifulco, B. A. Fox, and T. M. Beer, "Sustained complete response to CTLA-4 blockade in a patient with metastatic, castration-resistant prostate cancer," *Cancer Immunology Research*, vol. 2, no. 5, pp. 399–403, 2014.

[35] M. A. Spitz, G. Lenaers, M. Charif et al., "Paroxysmal dyskinesias revealing 3-hydroxy-isobutyryl-CoA hydrolase (HIBCH) deficiency," *Neuropediatrics*, vol. 52, no. 5, pp. 410–414, 2021.

[36] L. Marti-Sanchez, H. Baide-Mairena, A. Marcé-Grau et al., "Delineating the neurological phenotype in children with defects in the ECHS1 or HIBCH gene," *Journal of Inherited Metabolic Disease*, vol. 44, no. 2, pp. 401–414, 2021.

[37] J. Wang, Z. Liu, M. Xu et al., "Cinical, metabolic, and genetic analysis and follow-up of eight patients with HIBCH mutations presenting with Leigh/Leigh-like syndrome," *Frontiers in Pharmacology*, vol. 12, article 605803, 2021.

[38] G. Schottmann, A. Sarpong, C. Lorenz et al., "A movement disorder with dystonia and ataxia caused by a mutation in the HIBCH gene," *Movement Disorders*, vol. 31, no. 11, pp. 1733–1739, 2016.

[39] H. Peters, N. Buck, R. Wanders et al., "ECHS1 mutations in Leigh disease: a new inborn error of metabolism affecting valine metabolism," *Brain*, vol. 137, no. 11, pp. 2903–2908, 2014.

[40] Y. Zhang and L. Ma, "Identification of key genes and pathways in calcific aortic valve disease by bioinformatics analysis," *Journal of Thoracic Disease*, vol. 11, no. 12, pp. 5417–5426, 2019.

[41] A. Mazzone, M. C. Epistolato, R. De Caterina et al., "Neoangiogenesis, T-lymphocyte infiltration, and heat shock protein-60 are biological hallmarks of an immunomediated inflammatory process in end-stage calcified aortic valve stenosis," *Journal of the American College of Cardiology*, vol. 43, no. 9, pp. 1670–1676, 2004.

[42] M. Olsson, C. J. Dalsgaard, A. Haegerstrand, M. Rosenqvist, L. Rydén, and J. Nilsson, "Accumulation of T lymphocytes and expression of interleukin-2 receptors in nonrheumatic stenotic aortic valves," *Journal of the American College of Cardiology*, vol. 23, no. 5, pp. 1162–1170, 1994.

[43] N. Coté, A. Mahmut, Y. Bosse et al., "Inflammation is associated with the remodeling of calcific aortic valve disease," *Inflammation*, vol. 36, no. 3, pp. 573–581, 2013.

[44] J. Natorska, G. Marek, J. Sadowski, and A. Undas, "Presence of B cells within aortic valves in patients with aortic stenosis: relation to severity of the disease," *Journal of Cardiology*, vol. 67, no. 1, pp. 80–85, 2016.

[45] C. M. Crosby and M. Kronenberg, "Tissue-specific functions of invariant natural killer T cells," *Nature Reviews Immunology*, vol. 18, no. 9, pp. 559–574, 2018.

[46] L. Wu and L. Van Kaer, "Natural killer T cells and autoimmune disease," *Current Molecular Medicine*, vol. 9, no. 1, pp. 4–14, 2009.

[47] P. Ohukainen, S. Syväranta, J. Näpänkangas et al., "MicroRNA-125b and chemokine CCL4 expression are associated with calcific aortic valve disease," *Annals of Medicine*, vol. 47, no. 5, pp. 423–429, 2015.

[48] D. A. Hägg, F. J. Olson, J. Kjelldahl et al., "Expression of chemokine (C-C motif) ligand 18 in human macrophages and atherosclerotic plaques," *Atherosclerosis*, vol. 204, no. 2, pp. e15–e20, 2009.

[49] C. S. Kim, J. H. Kang, H. R. Cho et al., "Potential involvement of CCL23 in atherosclerotic lesion formation/progression by the enhancement of chemotaxis, adhesion molecule expression, and MMP-2 release from monocytes," *Inflammation Research*, vol. 60, no. 9, pp. 889–895, 2011.

[50] D. Wang, T. Xiong, W. Yu et al., "Predicting the key genes involved in aortic valve calcification through integrated bioinformatics analysis," *Frontiers in Genetics*, vol. 12, article 650213, 2021.

[51] D. MacGrogan, B. Martínez-Poveda, J. P. Desvignes et al., "Identification of a peripheral blood gene signature predicting aortic valve calcification," *Physiological Genomics*, vol. 52, no. 12, pp. 563–574, 2020.

[52] Y. Molad, N. Levin-Iaina, M. Vaturi, J. Sulkes, and A. Sagie, "Heart valve calcification in young patients with systemic lupus erythematosus: a window to premature atherosclerotic vascular morbidity and a risk factor for all-cause mortality," *Atherosclerosis*, vol. 185, no. 2, pp. 406–412, 2006.

[53] K. K. Teo, D. J. Corsi, J. W. Tam, J. G. Dumesnil, and K. L. Chan, "Lipid lowering on progression of mild to moderate aortic stenosis: meta-analysis of the randomized placebo-controlled clinical trials on 2344 patients," *Canadian Journal of Cardiology*, vol. 27, no. 6, pp. 800–808, 2011.